



UPPSALA
UNIVERSITET

*Digital Comprehensive Summaries of Uppsala Dissertations
from the Faculty of Science and Technology 1780*

Graphene Based Inks for Printed Electronics

MAN SONG



ACTA
UNIVERSITATIS
UPSALIENSIS
UPPSALA
2019

ISSN 1651-6214
ISBN 978-91-513-0588-2
urn:nbn:se:uu:diva-377697

Dissertation presented at Uppsala University to be publicly examined in Högssalen, Ångströmlaboratoriet, Lägerhyddsvägen 1, Uppsala, Thursday, 25 April 2019 at 09:00 for the degree of Doctor of Philosophy. The examination will be conducted in English. Faculty examiner: Doctor Anwar Ahnizay (RISE- Research Institutes of Sweden).

Abstract

Song, M. 2019. Graphene Based Inks for Printed Electronics. *Digital Comprehensive Summaries of Uppsala Dissertations from the Faculty of Science and Technology* 1780. 64 pp. Uppsala: Acta Universitatis Upsaliensis. ISBN 978-91-513-0588-2.

The outstanding properties of graphene make it attractive ink filler for conductive inks which plays an important role in printed electronics. This thesis focuses on the ink formulation based on graphene and graphene oxide (GO).

Liquid phase exfoliation of graphite is employed to prepare graphene dispersions, i.e., shear- and electrochemical exfoliation. High concentration graphene dispersions with small size, few-layer graphene platelets are obtained by both methods. With the addition of ethyl cellulose stabilizer, shear-exfoliated graphene platelets in NMP were successfully inkjet printed on different substrates. The printed graphene film with electrical conductivity of $\sim 3 \times 10^4$ S/m was obtained after annealing at 350 °C for one hour. Alternatively, the electrochemically exfoliated graphene nano-platelets were collected and redispersed in DMF to form inks. The printed film of conductivity $\sim 2.5 \times 10^3$ S/m was obtained after annealing at 300 °C for one hour.

Water based GO/Ag hybrid inks were developed for screen printing. When high concentration GO aqueous dispersion was mixed with reactive silver ink, the viscosity of the mixture increased instantly to above 1000 cP as a result of reactions between oxygen functional groups (OFGs) on GO sheets and ingredients in the reactive silver ink. When the screen printed lines with different GO:Ag ratios were annealed in air, the conductivity of the resultant reduced graphene oxide/silver nanoparticles (RGO/AgNP_x) composites decreased as silver content increased. As oxygen enriched compounds in RGO/AgNP_x composites were detected, we proposed that AgOx compounds were generated on the AgNPs surface, which raised the contact resistance between AgNPs and RGO flakes. To solve this problem, the printed patterns were instead annealed in reducing gas (Ar/H₂ 5%). The electrical conductivity $\sim 2.0 \times 10^4$ S/m was then achieved.

Furthermore, the reduction of GO using ammonium formate as reducing reagent was investigated. When applying a hydrothermal method, ammonium formate shows excellent reduction ability, surpassing the widely used reducing agent, L-ascorbic acid, under same condition. Elemental analysis shows the C/O ratio of RGO as high as ~ 11 and most OFGs were removed in the reduction process. Meanwhile, incorporated nitrogen atoms introduced active sites in resultant RGO, making it a promising electrocatalyst for oxygen reduction reaction.

Keywords: Exfoliation, Graphene inks, Inkjet printing, Screen printing, GO/Ag hybrid inks, Leuckart reaction, Reduction.

Man Song, Department of Engineering Sciences, Solid State Electronics, Box 534, Uppsala University, SE-75121 Uppsala, Sweden.

© Man Song 2019

ISSN 1651-6214

ISBN 978-91-513-0588-2

urn:nbn:se:uu:diva-377697 (<http://urn.kb.se/resolve?urn=urn:nbn:se:uu:diva-377697>)

Like dissolves like.

To myself ten years ago

List of Papers

This thesis is based on the following papers, which are referred to in the text by their Roman numerals.

- I S. Majee, **M. Song**, S-L. Zhang, Z-B. Zhang, (2016) Scalable inkjet printing of shear-exfoliated graphene transparent conductive films, *Carbon*, 102:51-57.
- II F-J. Miao, S. Majee, **M. Song**, S-L. Zhang, Z-B. Zhang, (2016) Inkjet printing of electrochemically-exfoliated graphene nanoplatelets, *Synthetic Metals*, 220:318-322.
- III **M. Song**, J. Zhao, H. Grennberg, Z-B. Zhang, (2018) Screen Printed Conductive Composites with Reduced Graphene Oxide and Silver, 2018 IMAPS Nordic Conference on Microelectronics Packaging (NordPac), 12-14 June, 2018, *IEEE Xplore*, DOI: 10.23919/NORDPAC.2018.8423856.
- IV **M. Song**, L. Tahershamsi, J. Zhao, Z-B. Zhang, H. Grennberg, (2018) Rapid gelation of aqueous graphene oxide induced by sonication-promoted Leuckart reaction, *ChemNanoMat*, 4: 1145-1152.
- V **M. Song**, J. Zhao, L. Riekehr, H. Grennberg, Z-B. Zhang, (2018) Nitrogen-doped Reduced Graphene Oxide Hydrogel Achieved via a One-Step Hydrothermal Process, submitted.

Reprints were made with permission from the respective publishers.

Author's contributions

- I Minor part of planning, setup assembly, experiments, and data analysis, discussion with coauthors
- II Minor part of planning, setup assembly, experiments, and data analysis, discussion with coauthors
- III Major part of planning, experiments, data analysis, and manuscript writing
- IV Major part of planning, most of experiments, data analysis, and manuscript writing
- V All of the planning, most of experiments, data analysis, and majority of manuscript writing

List of Related Contributions

Related papers which are not included are listed below.

- I P. Ahlberg, M. Hinnemo, **M. Song**, X. Gao, J. Olsson, S-L. Zhang, Z-B. Zhang, (2015) A two-in-one process for reliable graphene transistors processed with photo-lithography, *Applied Physics Letters*, 107(20): 203104.

- II J. Zhao, **M. Song**, C-Y. Wen, S. Majee, D. Yang, B. Wu, S-L. Zhang, Z-B. Zhang, (2017) Microstructure-Tunable Highly Conductive Graphene-Metal Composites Achieved by Inkjet Printing and Low Temperature Annealing, *Journal of Micro-mechanics & Microengineering*, 2017, 28 (3).

Contents

Scope of the thesis	13
1. Introduction.....	15
1.1 Printed Electronics	15
1.2 Printing techniques and inks.....	16
1.2.1 Printing techniques	16
1.2.2 Inks for printing	19
1.3 Graphene inks.....	22
1.3.1 Production of high quality graphene.....	22
1.3.2 Mass production of graphene in liquids.....	23
1.3.3 Reduced graphene oxide.....	26
1.3.4 Graphene ink for printing	26
2. Graphene ink preparation.....	29
2.1 Graphene preparation by exfoliation of graphite.....	29
2.2 The reduction of GO	30
3. Characterization Techniques.....	33
3.1 Spectroscopy	33
3.2 Microscopy.....	37
3.3 Other characterization techniques	39
4. Overview of the appended papers.....	44
4.1 Graphene nano-platelet inks for inkjet printing.....	44
4.2 GO based inks for screen printing.....	46
4.3 GO gelation	50
4.4 GO reduction	51
5. Concluding Remarks and Outlook.....	53
5.1 Concluding remarks	53
5.2 Outlook.....	54
Sammanfattning på svenska.....	55
Acknowledgement	57
Reference	59

Abbreviations and Symbols

2D	Two-Dimensional
3D	Three-Dimensional
AFM	Atomic Force Microscopy
CNT	Carbon Nanotube
CV	Cyclic Voltammetry
CVD	Chemical Vapor Deposition
DMF	Dimethylformamide
DOD	Drop-On-Demand
EM	Electron Microscope
FET	Field-Effect Transistor
FTIR	Fourier Transform Infrared
GO	Graphene Oxide
GO/Ag	Graphene Oxide/Silver
HRTEM	High-Resolution Transmission Electron Microscopy
HOPG	Highly Oriented Pyrolytic Graphite
IR	Infrared
ITO	Indium Tin Oxide
MWCNT	Multi-walled Carbon Nanotube
NMP	N-methyl-2-pyrrolidone
NP	Nano Particle
NRGO	Nitrogen-doped Reduced Graphene Oxide
OFG	Oxygen Functional Groups
ORR	Oxygen Reduction Reaction
PE	Printed Electronics
RDE	Rotating Disk Electrode
RGO	Reduced Graphene Oxide
SAED	Selected Area Electron Diffraction
SEM	Scanning Electron Microscopy
EDS	Energy-dispersive X-ray spectroscopy
TCF	Transparent Conducting Film
TEM	Transmission Electron Microscopy
TGA	Thermogravimetric Analysis
UHV	Ultra-high Vacuum
XRD	X-ray Diffraction
XPS	X-ray Photoelectron Spectroscopy

d	Crystal lattice spacing
δ_G	Square root of surface energy of graphene
δ_{sol}	Square root of surface energy of solvent
ϕ	Graphene volume fraction
$E_{S,G}$	Surface energy of graphene
$E_{S,L}$	Surface energy of liquid (solvent)
η	Liquid viscosity
L	Flake length of graphene
I_D	Intensity of D-band of Raman spectrum
I_G	Intensity of G-band of Raman spectrum
n	Diffraction order
R_s	Sheet resistance
S	Siemens
s	Probe distance
T	Temperature
T_{flake}	Flake thickness of exfoliated graphene
λ	X-ray wavelength
θ	Diffraction angle
σ_0	Stress
ε_0	Strain
δ	Phase change
G'	Storage modulus
G''	Loss modulus
ΔG_{MIX}	Free energy for mixing
ΔH_{MIX}	Enthalpy of mixing
ΔS_{MIX}	Entropy of mixing
$\dot{\gamma}$	Shear force

Scope of the thesis

As printed electronics is finding new commercial opportunities, the demand for conductive inks keeps growing to meet emerging requirements. Due to its outstanding properties, graphene shows great potential as alternative conductive ink filler. With this background, my project is to develop graphene-based conductive inks for printing interconnects and electrodes in electronic devices. This thesis is based on the research results for this project and is structured in the following way:

In Chapter 1, the background, motivation and state-of-art of graphene-based inks will be briefly introduced. In the following chapter, fundamentals related to my research are discussed. Chapter 3 describes the characterization techniques for measurements and result analysis. Chapter 4 is a summary of the included papers, which goes as following:

The first section (**Paper I and II**) focuses on the preparation of graphene by liquid phase exfoliation of graphite in organic solvents or inorganic salt electrolyte. Small size and few layer graphene platelets are successfully prepared and subsequently used for inkjet printing. It is found that inkjet printing of graphene inks suffers from some severe problems such as low efficiency. Additionally, inkjet printing requires strict control of the graphene flake size because oversized flakes will clog the printing nozzles. To solve these problems, we alternatively turn to graphene oxide and screen printing. A GO dispersion mixed with water based reactive silver ink is developed to increase the overall conductivity. This work that is partially published in **Paper III** and additional results are also presented in section 4.2. In the study of GO/Ag hybrid inks, we found that the viscosity increase instantly when GO dispersion was mixed with silver ink. The results are published in **Paper IV**—reduction induced gelation of GO dispersion via Leuckart reaction. This work inspired the further study on the reduction of GO using ammonium formate as reducing reagent by hydrothermal method. It is proved that ammonium formate possesses excellent reduction ability for GO and the incorporation of nitrogen atoms in resultant reduced graphene oxide endows it excellent electrocatalytic ability towards oxygen reduction reaction. The results are included in the last manuscript--**Paper V**.

The thesis ends with a short summary of my work and an outlook on future work.

1. Introduction

1.1 Printed Electronics

Printed electronics (PE) refers to the application of printing technologies for the fabrication of electronic circuits and devices on a variety of substrates. Traditionally, electronic devices are mainly manufactured by silicon (Si) technology relying on photolithography and vacuum techniques which require clean room facilities and thus inevitably high cost. Compared to these multi-staged, expensive, and wasteful methods in Si electronics, printing offers a rapid and cost-effective way of additively manufacturing electrical circuits on various substrates. Furthermore, by combining printing technology and a broad range of materials like conductive polymers, carbon materials and inorganic materials, PE enables the realization of thin, lightweight and large-area electronics.

The PE market has been growing fast and is estimated to reach USD 13.6 billion by 2023 from USD 6.8 billion in 2018.[1] Current market drivers mainly include printed flexible displays[2], flexible batteries[3, 4], printed organic solar cells[5], sensor arrays[6], and radio frequency identification tags (RFID)[7]. Figure 1.1 shows the estimated market share for printed, flexible, and organic electronics in 2018. It is worth noting the large overlap between these three fields.

Originally, PE was related to organic or plastic electronics that used one or more inks made of carbon-based compounds. However today, as the market for PE grows, printing technologies and ink materials for manufacturing electronics have evolved fast to meet the market's needs. Especially the fast development of nanomaterials accelerates the evolution of PE products. In the past two decades, the synthesis processes, printing capabilities, electronic properties of nanomaterials-based inks have undergone tremendous advances.[8] As a result, great advances have been made in PE with the merging of printing technology and nanomaterials.

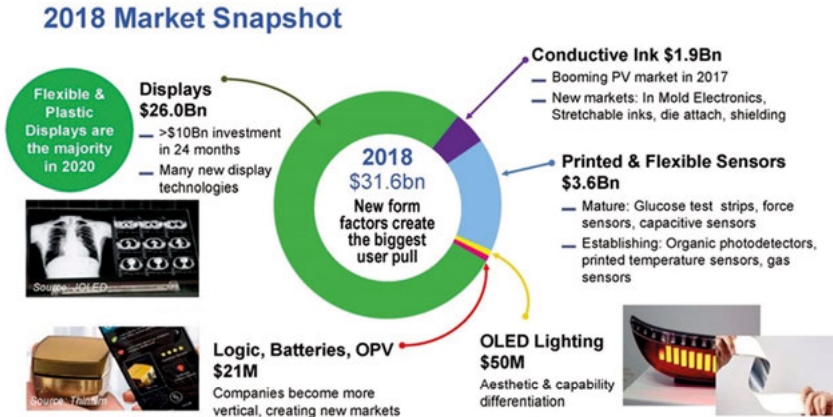


Figure 1.1 Market for printed, flexible, and organic electronics in 2018 (IDTechEx)[9]

1.2 Printing techniques and inks

Similar to conventional printing processes, manufacturing PE involves printing ink layers on substrates or on top of another. Almost all industrial printing methods could be used in PE, such as inkjet printing, screen printing, flexography, gravure, and offset lithography. While differently from conventional inks, ink materials for PE should fulfill certain electrical functionalities. Therefore, the essential tasks for PE are to develop printing technologies and ink materials that provide desired properties as well as to balance the performance with economics.

1.2.1 Printing techniques

Inkjet printing is one of the most commonly used printing technologies, which produces ink droplets from the fluid channel and deposits in target position. In PE production, the formation of ink droplets is realized by drop-on-demand (DOD) technology where droplets are only formed and ejected by a thermal or piezoelectric element when required, as shown in Figure 1.2a. The diameter of the ink droplets varies from 10 to 150 μm , which approximately corresponds to the diameter of the printing nozzle. The volume of the droplets is in the pico-liter range. Depending on its nature, inkjet printing has several advantages over other printing methods.

- It is flexible and versatile, and can be set up with relatively low effort. Figure 1.2b shows a picture of an inkjet printer in our lab.

- It is a non-contact and DOD process. A variety of materials could be selectively deposited onto desired position in a drop-by-drop manner, guaranteeing minimal ink consumption and material wastage.
- The mask- and master-less nature makes it suitable for a wide range of production scales, from prototyping to large-scale industrial production.
- It is flexible with regard to its positioning within a process chain. It is possible to add functionalities using inkjet printing on a substrate that already has electronic structures and devices fabricated by printing technology or using any other technologies.
- As a digital printing method, it allows a short turnaround time for device fabrication, especially suitable for lab-scale research.

With all above advantages mentioned, it is important to point out the main drawbacks of inkjet printing:

- It shows limitations in terms of available materials.[10] The size of functional materials, viscosity, and surface potential of inks should be controlled in a specific range for good printability.
- It normally suffers from low throughput for the mass-production of PE products compared to other printing technologies.

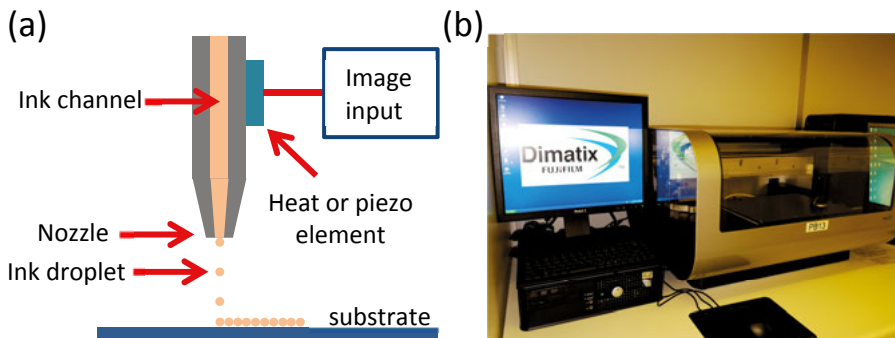


Figure 1.2 (a) Illustration of the working principle of inkjet printing and (b) photograph of a Dimatix inkjet printer.

Screen printing is a conventional low-cost printing technique that is also commonly used to manufacture PE products. As its name implies, this printing method relies on a screen functioned as mask, which is a woven piece of fabric stretched tightly over a frame. Certain areas of this fabric are coated with a non-permeable material and ink can be pushed through the remaining

open spaces onto a substrate with a squeegee, as shown in Figure 1.3. The advantages of screen printing include:

- The usual thickness of a screen-printed pattern is in the range of several tens of microns with a single pass of printing, which cannot be realized by other printing methods.
- The surface of the recipient does not have to be flat and that the ink can adhere to various materials, such as paper, textiles, glass, ceramics, and metal.
- It has better compatibility with a wide range of ink materials compared to inkjet printing.
- It is a low-cost technology. The cost of printing mask is offset by the high output.

The main drawbacks of screen printing include the needs for mask-the screen, waste of materials, and inevitable physical contact between the mask with target substrate. With these considerations, it is unsuitable for the rapid prototyping of devices.

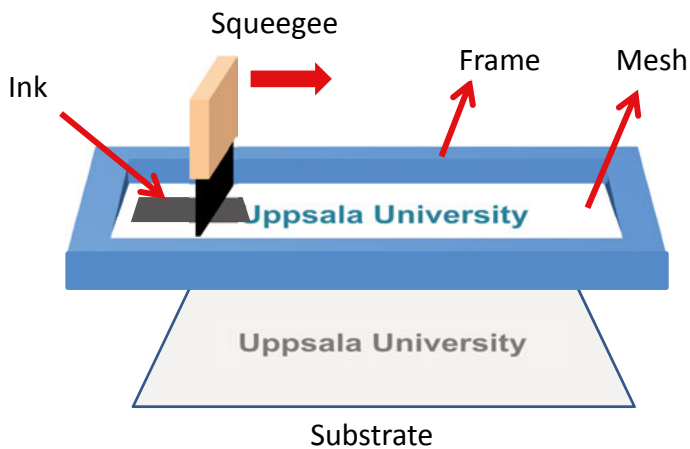


Figure 1.3 Illustration of screen printing.

This thesis mainly includes graphene-based ink formulation for both inkjet printing and screen printing. Other printing technologies such as *offset lithography* and *flexography* have also been investigated for manufacturing PE, but are still not as common as inkjet and screen printing.

In *offset lithography* a printing plate, which is most often made of aluminum, contains an image of the content that needs to be printed. When the plate is inked, only this image part holds ink. That inked image is subsequently transferred (or offset) from the plate to a rubber blanket and then to

the printing surface. The process can be used to print on paper, cardboard, plastic or other materials, but these have to have a flat surface.

In *flexography* (often abbreviated to *flexo*) the content that needs to be printed is on a flexible relief of a printing plate, which is made from rubber. This plate is inked and that inked image is subsequently transferred to the printing surface. The process can be used to print on almost any type of substrates such as papers, plastics, metals, and cellophanes.

1.2.2 Inks for printing

The other important element that plays a decisive role in the success of PE is the advancement in material development, that is, ink development. Ink materials should provide certain electrical functionalities e.g., conductivity, semiconductivity, resistivity, or dielectric property.

Amongst inks, vast interests have been drawn to conductive inks since all PE devices need electrodes and conductive structures. The printed conductive component is supposed to replace bulky wires in electrical circuits without losing too much of the performance. Conductive inks contain different conductive materials which can be classified into three categories from the material's point of view: metal-based ink such as Ag and Cu, conductive polymers, and carbon materials. The bulk properties of different ink materials are presented in Table 1.1. Each type of conductive materials offers unique properties suitable for particular applications.

For noble metal-based inks, two main types are commonly used. The first type is a suspension of nanoparticles, and is known as a nanoparticle (NP) ink.[11, 12] The second type of ink is known as metal-organic decomposition ink, an example of which involves a metal salt dissolved in a suitable solvent.[13-17] The NP ink usually has higher metal loads (thus high cost) as well as higher conductivity. The latter type is solution-based so it has advantages such as low curing temperature (<200 °C) and no nozzle clogging for inkjet printing. Silver is the most prevalent material for conductive ink due to its high conductivity and oxidation resistance. Copper inks have also been developed, but typically require core-shell nanoparticle designs or specialized photonic annealing treatments to produce conductive patterns[18]. Noble metal-based inks offer the highest conductivity among printed materials, but expensive precursors will raise the cost of PE products. The long-time (hours), high-temperature (>200 °C) sintering for nanoparticle-based ink is another concern, which sets limitation on the substrate choice.

Conductive polymers, such as PPV (polyphenylene vinylene) and PE-DOT:PSS (poly (3,4-ethylenedioxythiophene):poly (styrene sulfonic acid)), have also been developed for PE applications. Although they have much lower conductivity compared to metals, conductive polymers are attractive for PE due to their advantages such as solution processability, flexibility, light weight, and low-price. These materials offer a modest conductivity at

low cost, but they are limited in terms of chemical and thermal stability as all organic materials.

Functional materials in carbon inks include conventional carbon black or carbon nanomaterials such as fullerenes, carbon nanotubes (CNTs), and graphene. Carbon black-based inks of a wide range of electrical properties have been developed from low conductivity inks for antistatic packaging or coating to relatively high conductivity inks for electrodes. Fullerenes have poor electrical conductivity due to reduced π bond overlap.[19] However, they are excellent electron acceptors, thus functionalized fullerenes are considered promising n-type semiconductors. [20] CNTs and graphene both have excellent electronic and thermal properties. But when it comes to inks, the production and processing of CNTs are more complicated compared to graphene.[19] Plus, the CNT-to-CNT junctions and remaining impurities would lower the electrical conductivity of the printed structure by orders of magnitude, as compared to the conductivity of individual CNT. Graphene, as the youngest member in the nanocarbon family, has attracted vast attention in abroad range of areas due to its outstanding electronic, thermal, mechanical, and optical properties. Graphene-based inks offer a low-cost alternative with excellent environmental stability and desirable conductivity, making them suitable for a range of applications from thin-film transistors[21-24] and sensors[25-27] to supercapacitors[28, 29] and photovoltaics[30, 31]. Graphene inks have shown great potential that inspires a worldwide research, as well as this thesis work. The production and status of graphene inks will be introduced in next section.

Table 1.1 Electrical properties of different ink materials. MWCNT stands for multi-walled carbon nanotube.

Materials		Electrical properties	Notes
Metals	Ag	6.30×10^5	Bulk conductivity (S/cm)
	Cu	5.96×10^5	
	Au	4.10×10^5	
Organic polymer	PEDOT/PSS	$<10^4$	Doped conductive polymer conductivity (S/cm)
	PPV	<100	
Carbon	Carbon black	10-100	Sheet resistance Ω/\square of 25 μm thick film
	MWCNT	10^4 - 10^5	Conductivity (S/cm) of individual MWCNT
	Graphene	2×10^5 [32]	Intrinsic mobility (cm^2/Vs)

Beside the ink materials, other factors should also be taken into consideration for specific applications such as printability, viscosity, stability, and compatibility.[33] Therefore, whatever the conductive material or solvent is used, these inks will often contain other constituents such as dispersants, adhesion promoters, surfactants, thickeners, stabilizing agents and other additives.[34] Those additives will inevitably lower the electrical conductivity of printed structures, sometimes even by orders of magnitude compared to the intrinsic properties of ink materials.

Furthermore, the compatibility of inks with substrates, the required feature widths, and desired properties are also essential factors. Depending on the nature of the targeted PE products, one must make a suitable choice regarding the ink, substrate, designed device structure, pattern geometry, manufacturing speed, yield, quality, and production cost. Table 1.2 shows various printing techniques, requirement for inks and other printing parameters. In addition to aforementioned printing technologies, gravure, dispense, μ CP, and nanoimprint printing methods are also listed for comparison.

Table 1.2 Feature comparison of different printing methods[35]

Printing method	Ink viscosity (cP)	Line width (μ m)	Line thickness (μ m)	Speed (m/min)	Other feature
Inkjet	10–20 (electrostatic inkjet: Approx. 1,000)	30–50 (electrostatic inkjet: Approx. 1)	Approx. 1	Slow (rotary screen: 10 m/s)	Surface tension: 20–40 dyn/cm On demand Noncontact
Offset	100–10,000	Approx. 10	Several –10	Middle—fast Approx. 1,000	
Gravure	100–1,000	10–50	Approx. 1	Fast Approx. 1,000	
Flexo	50–500	45–100	<1	Fast Approx. 500	
Screen	500–5,000	30–50	5–100	Middle Approx. 70	
Dispense	1,000–10 ⁶	Approx. 10	50–100	Middle	Single stroke
μ CP	–	Approx. 0.1	Approx. 1	Slow	
Nanoimprint	–	Approx. 0.01	Approx. 0.1	Slow	

1.3 Graphene inks

Graphene is a 2D single-atom-thick layer of sp^2 hybridized carbons tightly bonded in a hexagonal lattice, equivalent to a single layer of graphite. It has attracted tremendous interest and research effort since it was first reported in 2004[36]. Its extreme mechanical strength, high charge carrier mobility, superlative thermal and chemical stability, and intrinsic flexibility make it promising for many applications.[36-40] The applications depend strongly on the quality of graphene, compatibility with other process as well as preparation cost. Figure 1.4 shows several ways to synthesize graphene for particular applications versus price. For conductive ink applications, high conductivity, excellent thermal stability, and layered structure make graphene a perfect option.

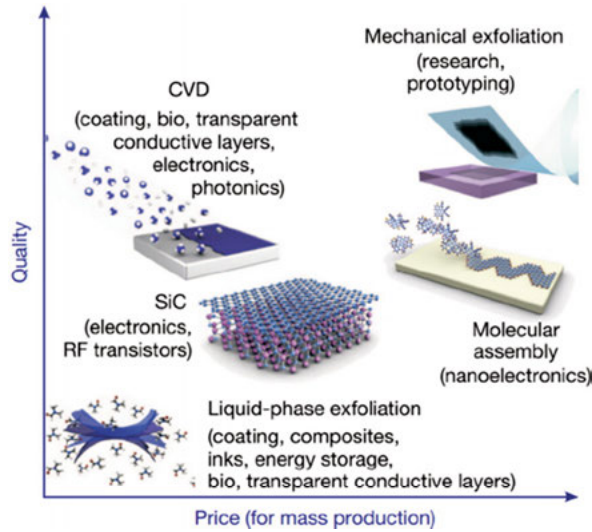


Figure 1.4 Methods of production of graphene. Reprinted with permission from [41], copyright (2012) Springer Nature.

1.3.1 Production of high quality graphene

High quality graphene usually can be obtained by three main methods, namely, mechanical exfoliation, chemical vapor deposition (CVD), and epitaxial growth.

The first reported graphene[36] was produced by mechanical exfoliation (repeated peeling) of small mesas of highly oriented pyrolytic graphite (HOPG), which also boosted the research of graphene and other 2D materials quickly. This method guarantees the intactness of pristine graphene, so it

is widely used to prepare devices for fundamental studies of graphene. However, this method is impossible to scale up, which limits its applications.

Soon after the first report on graphene, it was found that large-area uniform polycrystalline graphene films could be grown by CVD on nickel and copper foils or other catalytic substrates.[42-45] Here, the carbon source, such as methane, was in gas form. It is input to CVD furnace together with reducing agent hydrogen gas. This approach shows promise for many electronic applications despite the fact that the complete process typically requires transfer from the catalytic substrates to a dielectric surface or any other substrates of interest. The most common way to realize this transfer is to etch away the catalytic substrates, such as copper foils, which increases the process complexity and overall cost.

An alternative approach to CVD is via the thermal decomposition of silicon carbide (SiC)[46]. The SiC substrate is subjected to heating in ultra-high vacuum (UHV) to temperature between 1273 and 1773 K, which causes Si to sublimate, leaving a carbon-rich surface.[47]

The graphene produced by the above mentioned three methods has small number of defects and thus good properties that are close to pristine graphene which is desirable for applications in electronic devices. However, the high temperature, time- and energy-consuming process of CVD and thermal decomposition growth is an obstacle to applying as-prepared graphene for electronics.

1.3.2 Mass production of graphene in liquids

Exfoliating graphite in liquids is a common and cost-effective way to mass produce graphene. It is noteworthy that unusually we call the product "graphene" when the graphitic layers $N < 10$, specifically, "monolayer graphene" with $N=1$, "few-layer graphene" with $N=2$ to 4, "multiple layer graphene" with $N=5$ to 10, and "graphite" when $N=10$ and beyond.

The essence of graphite exfoliation in liquids is to overcome the van der Waals forces between the adjacent graphene layers.[48] Therefore, introducing additional external forces or/and hetero atoms/chemicals to overcome the attractive van der Waals interactions are common ways. To date, graphene in liquid has been successfully prepared by (1) sonication[49, 50], (2) wet ball milling[51], (3) shear[52-54] and (4) electrochemical[53, 55-58] exfoliation.

Due to the hydrophobic nature of graphene, exfoliating graphite in water is particularly challenging, but it is feasible with the aid of surfactants. Lotya *et al.*[49] reported the first sonication-based exfoliation of graphite in water using sodium dodecyl benzene sulfonate as surfactant. However, the concentration is far too low (< 0.01 mg/mL) for real applications. Since then, a variety of surfactants have been investigated including cetyltrimethylammonium bromide[59], sodium cholate[60], sodium deoxycholate bile salts[61], and bolaamphiphile[62]. The typical concentration of prepared graphene

dispersion is on the order of 0.1 mg/mL which is still too low. A thorough study on surfactant-aided exfoliation of graphite in water by Guardia *et al.* demonstrated that non-ionic surfactants could efficiently facilitate the exfoliation process. The best result, ~ 1 mg/mL, was achieved by using the triblock copolymer Pluronic[®] P-123.[63]

The surfactant-free exfoliation of graphite in a range of organic solvents was also achieved by sonication.[50] It is proved that the exfoliation can occur more easily when the surface energy of solvents are close to that of graphene. This work provides the theoretical basis for the solvent selection for graphite exfoliation and the mechanisms will be addressed in Chapter 2.1. Though this method suffers from a severe drawback, low concentration (~ 0.01 mg/mL), it opens a new vista for the mass production of graphene. Based on the same idea, high concentration graphene dispersion could be achieved by prolonging sonication time[64], adding surfactants and polymers[65-67], and solvent exchange methods[68, 69].

In the sonication method, the induced strong cavitation acts on graphite surfaces, helping to overcome the van der Waals forces between graphene layers. In contrast, shear force is also utilized to exfoliate graphite like by ball milling[51, 70], employing a vortex fluidic film in rapidly rotating tube[53] or using a high-shear rotor-stator mixer[52]. The main drawbacks of wet ball milling include the long processing time (several tens of hours) and the low exfoliation degree, which hinders its practical applications. The vortex fluidic exfoliation uses low concentration graphite dispersion (0.1 mg/mL) as starting material due to the limitation of the setup. As a result, the graphene output is very low. Compared to wet ball milling and vortex fluidic film methods, exfoliation of graphite by a high-shear mixer shows greater potential for graphene production. It is easy to scale up and the graphene concentration is tunable by adjusting the operation parameters such as rotating speed, vessels, and time. The instrument for shear exfoliation and as-prepared graphene are shown in Figure 1.5.

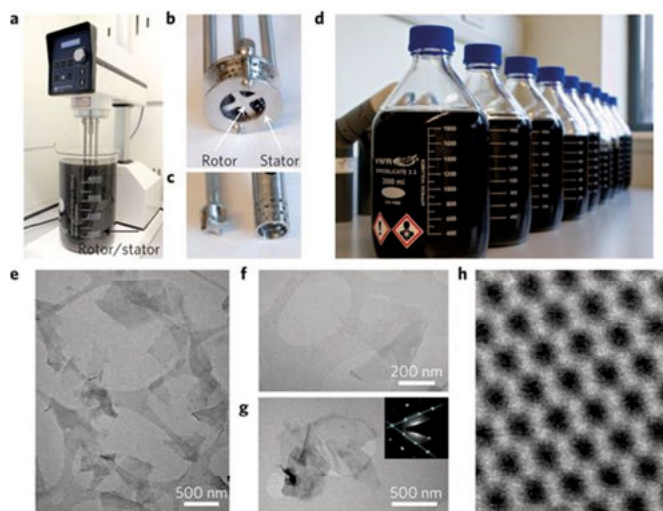


Figure 1.5 (a-d) Production of graphene by shear mixing; (e-h) TEM analysis of as-prepared graphene. Reprinted with permission from [52]. Copyright (2014) Springer Nature.

Another potential method for mass production of graphene is electrochemical exfoliation which is realized by applying a voltage to graphite rod/Pt wire (electrodes) in ionic-liquid/water solution (electrolyte), [55, 56, 58, 71] as shown in Figure 1.6. By this method, heteroatom (S, O) or molecule functionalized graphene can be achieved in contrast to the pristine graphene flakes produced by mechanical exfoliation. The advantages of electrochemical exfoliation include high output, easy implementation of setup, and ability for functionalization.

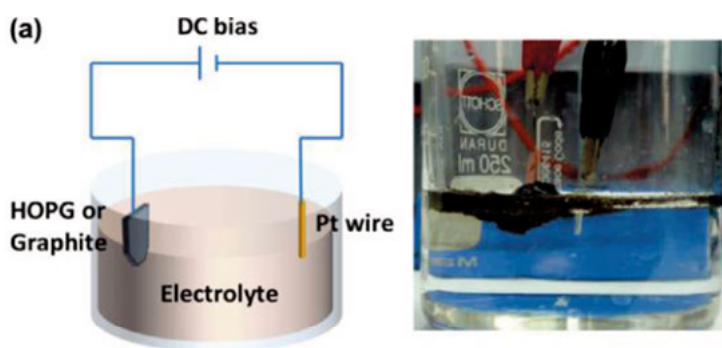


Figure 1.6 Schematic illustration and photo for electrochemical exfoliation of graphite. Reprinted with permission from [55]. Copyright (2011) American Chemical Society.

1.3.3 Reduced graphene oxide

The above described approaches yield pristine graphene of relatively good quality (compared to mechanically peeled graphene from HOPG) although a small number of defects are also introduced. In contrast, another method relies on the oxidization-reduction process in which a large number of defects are introduced on purpose in the oxidation process. Firstly, oxidized graphite is derived from graphite by treatment in strong acids, where oxygen functional groups (OFGs) are incorporated onto the graphitic lattice. The OFGs make oxidized graphite hydrophilic and thus could be dispersed in solvents like water. The single layer GO could be readily achieved when oxidized graphite is dispersed in water. After a following reduction step, the OFGs are (partially) removed so that the properties of graphene can be (partially) restored. This method has attracted wide interest due to its high yield, easy process and compatibility with functionalization by other materials. The disadvantage falls on the difficulty to fully restore the properties of graphene. Thermal annealing and chemical reduction are the two most popular approaches to reduce GO. A decent degree of reduction of GO could be achieved by thermal annealing at $>700\text{ }^{\circ}\text{C}$, where using an inert or reducing gas could yield even better results. [72-75] On the other hand, GO have been reduced chemically by reducing agents like L-ascorbic acid[76], hydrazine [77], sodium borohydride[78], reducing sugars[79], and hydrohalic acids[80] as well. However, some reductants are toxic and are not easy to handle, some are mild but only show limited reduction effect. More details will be discussed in Chapter 2.2.

1.3.4 Graphene ink for printing

Stable and high-concentration graphene inks with suitable viscosity and solvent composition are desirable for printing. For this reason, both liquid phase exfoliated graphene and GO are commonly used to formulate graphene inks.

The preparation of graphene by exfoliating graphite has been realized by many methods in a broad range of solvents with or without additives. But only a small part is suitable for ink formulation. Another concern is the indispensable additives which are employed to prevent graphene flakes from aggregating and/or improve the ink printability. High temperature ($200\text{--}400\text{ }^{\circ}\text{C}$) annealing is often required to remove the additives, which makes it not applicable to heat-sensitive substrates like papers and textiles. Therefore, careful selection of additives is very important. To date, most graphene inks use ethyl cellulose as stabilizer for inkjet printing[65, 69, 81], gravure printing[82] and screen printing[83]. Though shear and electrochemical exfoliation methods show great potentials for the efficient production of high concentration graphene dispersion, it had not been used to make graphene inks for inkjet printing before our work [84, 85].

Alternatively, GO dispersions are also popularly utilized to make inks due to their excellent processability and dispersibility in a broad range of solvents. There are reports on GO based inks for inkjet printing [22, 28, 86], 3D printing[87], and screen printing[88], but the electrical properties of printed structures are determined by the reduction level of GO and the restoration of graphitic lattice. The graphene inks and their electrical performance reported in recent years are summarized in Table 1.3. The electrical conductivities of commercial Ag inks and indium tin oxide (ITO) are also shown for comparison. Apparently, the electrical performance of graphene inks is much poorer than that of Ag inks and ITO. Considering the outstanding theoretical properties of pristine graphene, it deserves more investigations to the study of graphene inks.

Table 1.3. Electrical performance of various graphene inks made by different methods. Exf. G, EC, and TCF stands for exfoliated graphene, ethyl cellulose, and transparent conducting film respectively. The references marked with * are our work.

Materials	T(°C)	Rs kΩ/□ (T, transmittance)	Conductivity S/cm	Ref.
Sonication Exf. G/EC	250		~250	[65]
	250		100	[82]
	300		~200	[83]
	Photonic sintering	30	~100	[89]
	400	6 (75%)		[81]
	400	30 (80%)		[69]
Shear Exf. G/EC	350	0.26 (86%)	400	[84]*
Electro- chemical Exf. G	300	0.9 (53%)	25	[85]*
Supercritical CO ₂ Exf. G	300		92	[90]
Dense G nanoflake	100		430	[91, 92]
RGO nanowire	400, vacuum		11.3	[87]
RGO	200	300		[24]
	L-ascorbic acid, 80		15	[27]
	400		9	[26]
	UV	>1		[86]
	Photonic sintering	1000	<0.5×10 ⁻²	[93]
Ag	~200		10 ⁴ -10 ⁵	
ITO		<0.1 (>90%)	~10 ⁴	TCF

2. Graphene ink preparation

2.1 Graphene preparation by exfoliation of graphite

As it was outlined in Chapter 1, the essence of exfoliation of graphite in liquid phase is to overcome the van der Waals force and stabilize the exfoliated graphene sheets. Due to their similarities, the exfoliation of graphite was much inspired by previous studies on the dispersion of CNTs, such as in organic solvents and in aqua solutions with appropriate surfactants. In 2008, Prof. Jonathan N. Coleman's group reported on exfoliation of graphite by sonication in several solvents. In the following years, there were a series of studies on this topic from his group as well as other groups [67, 94, 95] including ours. The main issues related to the mechanism are summarized here.

Whether or not the exfoliation can happen is determined by the free energy of mixing, ΔG_{MIX} (J/m³) which is the difference in free energy between a mixture of two components and the two components in their unmixed form.[96]

$$\Delta G_{MIX} = \Delta H_{MIX} - T\Delta S_{MIX} \quad (2.1)$$

where ΔH_{MIX} (J/m³) is the enthalpy of mixing and ΔS_{MIX} (J/m³·K) is the entropy of mixing. If ΔG_{MIX} is negative, mixing is favorable. For solutions of macromolecules such as polymers in solvents, ΔS_{MIX} has a small positive value arising from increased conformational mobility of the polymer chains. This means that for mixing to occur, ΔH_{MIX} must be below a critical value, which is relatively small. It has been demonstrated that the enthalpy of mixing for graphite is minimized when the surface energy of solvents are close to that of graphene (~ 68 mJ/m²), which is given by,[50]

$$\frac{\Delta H_{mix}}{V_{mix}} \approx \frac{2}{T_{flake}} \left(\delta_G - \delta_{Sol} \right)^2 \phi \quad (2.2)$$

Where $\delta_i = \sqrt{E_{sur}^i}$ is the square root of the surface energy (J/m²) of phase i (i denotes solvent or graphite), T_{flake} is the thickness (m) of graphene flake

and ϕ is the graphene volume fraction ($1/\text{m}^3$). [50] For graphite, the surface energy is defined as the energy per unit area required to overcome the van der Waals forces when peeling two sheets apart, while the solvent surface energy is related to the surface tension and surface entropy. It is expected a minimal energy cost of exfoliation for solvents whose surface energy matches that of graphene. A more general expression was further evolved based on Hildebrand and Hansen solubility parameters [96]. It has been proved that graphite could be exfoliated efficiently in solvents such as N-methyl-2-pyrrolidone (NMP), dimethylformamide (DMF), benzyl benzoate and so on.

By sonication graphite could be exfoliated in abovementioned solvents, but the overall efficiency ($< 0.4 \text{ g/h}$) and yield ($\sim 1 \text{ wt\%}$ of the start graphite) are still too low to put into real application. For example, to get a relative high concentration (1.2 mg/mL) graphene dispersion, it took up to 460 h [64]. But combined with this theory, shear exfoliation of graphite in certain solvents was further developed and has shown great success in mass production of graphene. [52, 53] Their systematical study proved that as long as the shear rate $\dot{\gamma}_{\min} > 10^4 \text{ s}^{-1}$, graphite could be exfoliated. The shear rate is given by: [52]

$$\dot{\gamma}_{\min} = \frac{[\sqrt{E_{S,G}} - \sqrt{E_{S,L}}]^2}{\eta L} \quad (2.3)$$

Where $E_{S,G}$ and $E_{S,L}$ are the surface energies (J/m^2) of graphene and liquid, η is the liquid viscosity ($\text{Pa}\cdot\text{s}$) and L is the flake length (m). This equation clarifies two points: the first is that the exfoliation energy is minimized for solvents with surface energies matching that of graphene and the other is that the flake size is reversely related to the shear rate.

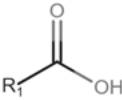
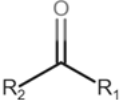
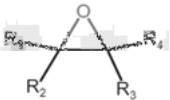
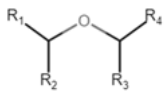
2.2 The reduction of GO

Two additional potential ways to mass produce graphene, electrochemical exfoliation of graphite and graphite-oxidation-reduction methods, both involve the introduction and removal of OFGs. On one hand, the OFGs make graphene sheets hydrophilic and thus more compatible with liquid processing. On the other, the incomplete removal of OFGs deteriorates the properties of graphene. Therefore, the removal of OFGs, or so called reduction is a vital and challenging issue. The electrochemically exfoliated graphene has less numbers of OFGs than GO, but encounters same problem, i.e., impossible to complete remove OFGs, when it comes to the reduction. So here I will use GO for the discussion of reduction.

Oxidized graphite was firstly reported in 1840 by Schafhaeutil [97] and 1859 by Brodie [98]. Currently the preparation method evolved from Hummers and Offeman's report [99] is the mostly used method which involves

treating graphite with concentrated strong acids (sulfuric acid and phosphoric acid) and subsequent potassium permanganate (KMnO₄), followed by cleaning process. During this process, OFGs will be introduced to the graphitic planes. Though the nonstoichiometric structure of GO is still in debate (even by same method, the composition varies from batch to batch), the mostly agreed OFGs includes five main types: hydroxyl group (-OH) and epoxides (-O-) decorated on the carbon basal plane, carboxylic acid group (-COOH), carbonyl groups (-C=O) on the sheet edges, and ether group.[100, 101] The chemical structures of the five OFGs are contained in Table 2.1. To restore the properties of graphene, GO must be reduced by removing the OFGs thermally or chemically. However, neither way could remove OFGs completely except for thermal annealing above 2000 °C in inert gas atmosphere[75].

Table 2.1 Five main oxygen functional groups on GO sheets

Hydroxyl	Carboxylic acid	Carbonyl	Epoxide	Ether
R_1-OH				

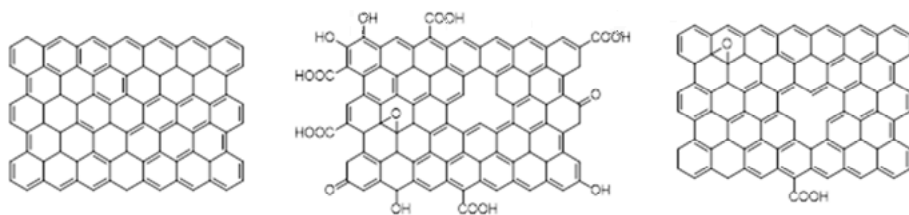


Figure 2.1 Illustrations of graphene, graphene oxide, and reduced graphene oxide (from left to right).

Among the various studies on reduction of GO, the report on mechanism is relatively less due to the complexity of chemical reactions and lack of means to directly monitor reduction processes. As a result, the understanding on the reduction mechanism mainly relies on computer calculation and simulation. For example, Kim *et al.* obtained the binding energy of an epoxy group is

much larger than a hydroxyl group when attached to 32-carbon-atom graphene[102], indicating epoxy groups are much more stable than hydroxyl groups. Another group studied the reduction of GO thermally and chemically by hydrazine via the density functional theory method and proves that epoxide groups and carbonyl groups are stable even when thermally treated at 700-1200 °C, while other OFGs could be removed.[103] In contrary, Jeong *et al.*[104] investigated the thermal stability of GO under mild heating (<200 °C) in low-pressure argon and found that such heat treatment removed hydroxyl and carboxyl groups as well as a part of the epoxides. Bagri *et al.*[105] studied the atomistic structure of progressive RGO by molecular dynamics simulation and found that the reduction progress was closely related to the OFG density.

Compared to thermal reduction, chemical reduction of GO could be realized at low or moderate temperatures with the aid of reducing reagents. The reducing reagents selectively react with certain OFGs while inactive to the rest, as the above mentioned hydrazine. Though numerous reducing reagents have been proved to be able to reduce GO to different extent, the reduction mechanisms are still in lack of systematical research. Except for a few papers on the reduction of GO by hydrazine, most mechanisms were only proposed for different reducing reagents [76, 106-110]. Therefore, the full reduction of GO and the understanding on reduction mechanisms remain as challenges.

3. Characterization Techniques

3.1 Spectroscopy

Fourier Transform Infrared (FTIR) spectroscopy is one of the most common and widely used spectroscopic techniques. It is the study of the interaction of infrared (IR) light with matter, more specifically, the absorption of IR by molecules generating absorption spectra. More broadly, three main processes may occur when a molecule absorbs energy from external radiation and each process involves an increase of energy proportional to the energy of absorbed light. The first route is a rotational transition when the absorption of radiation leads to a higher rotational energy level. The second one is a vibrational transition which occurs by absorption of quantized energy that leads to an increased vibrational energy level. The third route involves electrons of molecules being raised to higher electron energies, which corresponds to the electronic transitions. It is important to point out that the energy is quantized according to selection rules and absorption of radiation causes a molecule to move to a higher internal energy state, i.e., excited state. For each type of transition, there are multiple possibilities for the different energy levels.

The energy required for each transition can be rated in the following order: electronic > vibrational > rotational, which differs by an order of magnitude. Rotational transitions occur at lower energies (longer wavelengths) that are insufficient to cause vibrational and electronic transitions. Higher radiation energies are required for vibrational (near infrared) and electronic transitions (ultraviolet region of the electromagnetic spectrum). IR radiation could induce vibrational and rotational transitions but it does not have enough energy for electronic transitions.

There are two prerequisites for successful IR absorption. The first criterion is a net change in dipole moment in a molecule as it vibrates or rotates. The second necessary condition is that the frequency of IR radiation must match a vibrational/rotational frequency within a molecule. In this thesis, FTIR was carried out to detect the OFGs on GO and GO hydrogel in **Paper IV**, RGO and nitrogen-doped RGO (NRGO) in **Paper V** using a Perkin-Elmer Spectrum 100 FTIR spectrometer.

Raman Spectroscopy a complementary technique to IR spectroscopy. Both technologies examine changes in vibration, rotation and other low-frequency modes at the molecular level. While FTIR spectroscopy measures the amount of IR light absorbed, Raman spectroscopy measures the amount

of light scattered. The two techniques are complementary in that they can tell different things about a molecule.

Raman Spectroscopy relies on inelastic scattering, or Raman scattering, of monochromatic light, usually from a laser in the visible, near infrared, or near ultraviolet range. The laser light interacts with molecular vibrations, phonons or other excitations in the system, resulting in the energy of the photons being shifted up or down. The shift in energy gives information about the vibrational modes in the system. It is a powerful tool for characterization of graphitic materials in terms of electron and phonon behavior. Figure 3.1 presents a typical Raman spectrum of graphite (**Paper V**) which exhibits one characteristic band (G band) at 1585 cm^{-1} ascribed to the first-order scattering of E_{2g} phonon of sp^2 carbons in the graphite lattice, and a very weak band at 1327 cm^{-1} (D band) ascribed to disorder in sp^2 -hybridized carbons that arises from breathing mode of k -point phonons of A_{1g} symmetry.

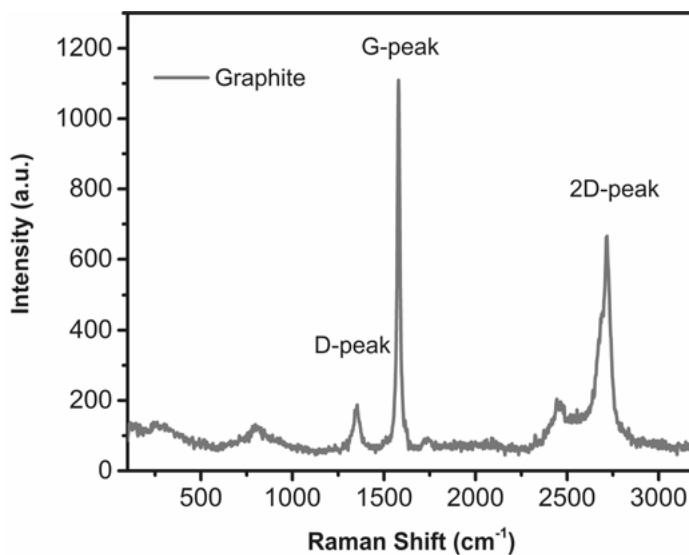


Figure 3.1 Typical Raman spectrum of graphite, laser wavelength of 532 nm. (**Paper V**)

By contrast, GO displays prominent D and G bands (Figure 3.2). The observed broadening of G band and blue-shift (1598 cm^{-1}), relative to those of graphite, is due to the doping induced by OFGs which determines the isolation of carbon double bonds that resonate at higher frequencies. At the same time, the increase in intensity of the D band indicates the creation of sp^3 domains due to the oxidation process. The D/G intensity (I_D/I_G) ratio is

widely used as a measure of the disorder of the graphene lattice, expressing the sp^2/sp^3 carbon ratio. Meanwhile, the I_D/I_G value varies inversely proportional to the average crystallite size in graphite materials due to the edge effect. Consequently, after GO reduction a slight increase of I_D/I_G relative to GO is noticed, suggesting the reduction in size of sp^2 domains, together with the increase in number. The changes suggest that, while sp^2 hybridization is recovered due to the reduction, the vacancies produced *via* carbon atom removal in the form of CO and CO₂ during graphite oxidation remain unchanged. Moreover, the position of the G and D peaks is shifted to opposite directions relative to GO, the fact attributed to graphitic “self-healing” and in-size reduction of aromatic clusters respectively.

Raman measurements were utilized to examine GO related samples through **all papers** by a Renishaw inVia confocal Raman microscope, with the laser wavelength of 532 nm.

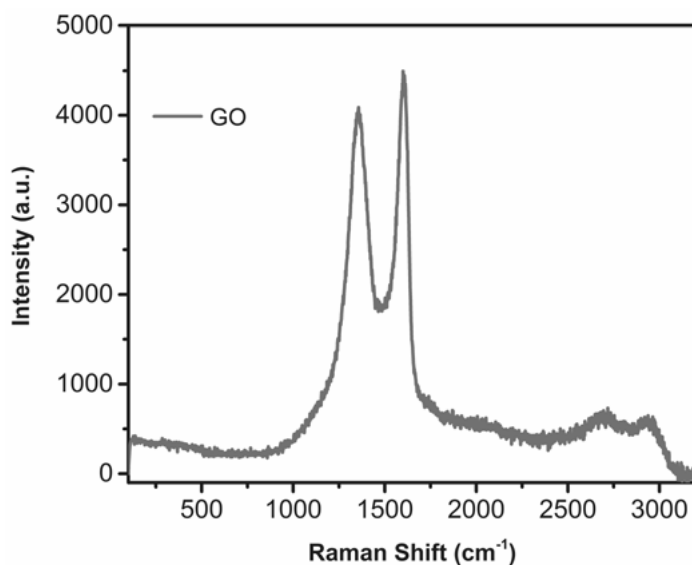


Figure 3.2 A typical Raman spectrum of GO. (**Paper V**)

The spectrum of electromagnetic radiation ranges from long-wavelength radio waves, to microwaves and infrared light, to visible light, to ultraviolet light, to higher energy X-rays, gamma rays and cosmic rays. Besides optical spectroscopy, X-ray technologies are also broadly used in material characterization such as *X-ray photoelectron spectroscopy* (XPS).

XPS is a surface-sensitive spectroscopic technique that measures the elemental composition, empirical formula, and chemical bonding state of the elements within a sample. XPS spectra are obtained by irradiating a beam of

X-rays on the material surface while simultaneously measuring the kinetic energy and number of photoelectrons that emit from the top few nanometers of the material. In contrast to the easy operation of the XPS instrument, attention should be paid to the interpretation of XPS spectra of carbon materials. For instance, the C 1s spectrum of carbon materials usually is a complex mixture of sp^2 and sp^3 carbon. High concentration of sp^2 carbon will have a broad, asymmetric peak with a tail towards higher binding energy. Plus, there would be one or more satellite features, several eV shift from the main C1s peak. The XPS C1s spectrum of HOPG is presented in Figure 3.3 as an example. Whereas, for high concentrations of sp^3 -bonded carbon such as diamond (Figure 3.3), the C1s peak will have a more symmetric shape and will also be slightly shifted to higher binding energy.

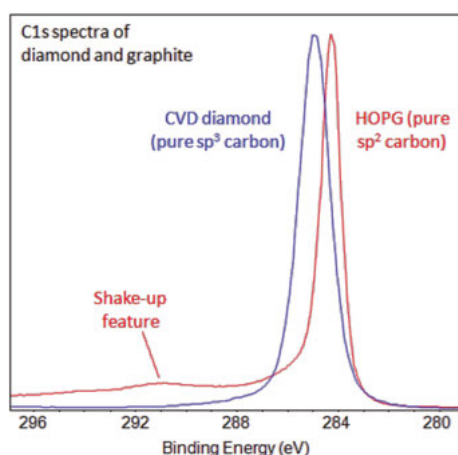


Figure 3.3 The XPS C1s spectra of diamond and HOPG[111]

Due to the large numbers of OFGs attached on GO sheets, the graphitic lattice is generally destroyed. Therefore, GO presents a C1s spectrum mainly containing sp^3 component. Whereas for RGO, some areas of sp^2 carbon are recovered, so the C 1s spectrum of RGO consists of overlapping sp^2 and sp^3 components. Thus de-convolution and peak fitting are required to analyze the chemical state of carbon. For example, sp^2 carbon should be fitted with asymmetric shape, including symmetric loss peaks where necessary. The sp^3 carbon and left OFGs should be fitted with symmetric peak shapes and the sp^3 carbon peak should be 1eV to the higher binding energy side of the sp^2 component.[111] Figure 3.4 shows a fitted C 1s spectrum of RGO from Paper V.

XPS measurements were performed with a Physical Electronics (PHI) Quantum 2000 Scanning ESCA Microprobe (Physical Electronics, Inc. Eden Prairie, Minnesota, USA) using monochromatic Al K α radiation ($h\nu=1486.6$ eV). XPS analysis was involved in **Paper II to V**.

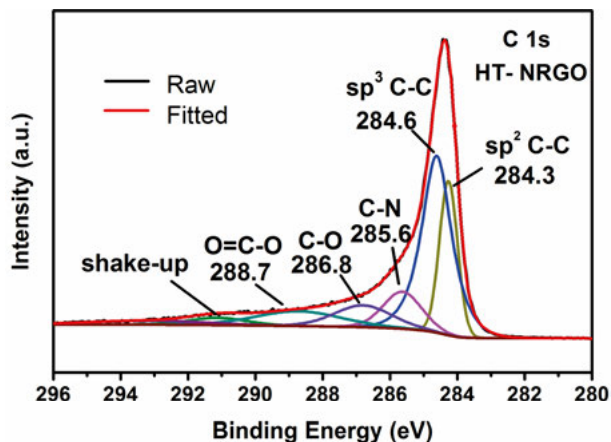


Figure 3.4 Peak fitted XPS C 1s spectrum of RGO (**Paper V**).

3.2 Microscopy

Electron Microscopy (EM) is an analytic technique that uses highly energetic electron beams instead of electromagnetic radiation to examine very fine objects. EM takes advantage of the much shorter wavelength of the electrons (e.g., $\lambda = 0.005$ nm at an accelerating voltage of 50 kV) compared to the wavelengths of visible light ($\lambda = 400$ nm to 700 nm).[112] When the accelerating voltage is increased in EM, the wavelength of electrons decreases and thus better resolution could be achieved.

Multiple signals will be generated when the high-energy electron beam interacts with the specimen, as shown in Figure 3.5. *Scanning Electron Microscopy (SEM)* collects the signals emitted from the specimen surface such as secondary electrons (for SEM images), diffracted backscattered electrons (to determine crystal structures and orientations), characteristic X-rays (for elemental analysis), Auger electrons (for elemental analysis of surfaces), and cathodoluminescence photos (for fundamental properties of matter such as bandgap, defects and so on). Among all the signals, secondary electrons are most valuable for showing morphology and topography of sample surfaces. Generated X-rays are characteristic to the elements within the sample and thus used for elemental analysis. For this thesis work, SEM characterization was performed using a field-emission gun high resolution SEM Zeiss Merlin

electron microscopy for samples in **Paper II to V**. SEM-EDS (Energy-dispersive X-ray spectroscopy) was carried out for elemental analysis in **Paper III**.

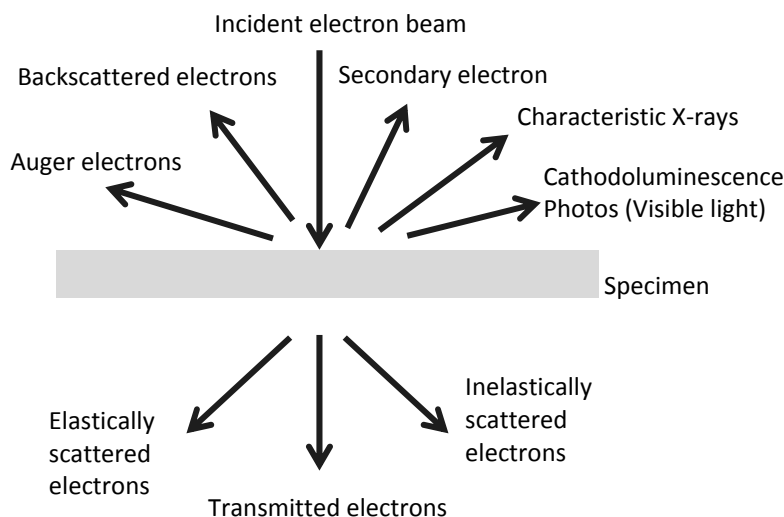


Figure 3.5 Signals generated when a high-energy electron beam interacts with a thin specimen.

Differently, *Transmission Electron Microscopy* (TEM) collects signals transmitted from an ultrathin specimen. Due to the higher accelerating voltages used in TEM, the image resolution of a TEM is generally better than that of a SEM. Hardware correction of spherical aberration for the high-resolution transmission electron microscopy (HRTEM) has allowed the production of images with resolution below 0.5 angstrom and magnifications above 50 million times.

Selected Area Electron Diffraction mode (SAED) is often used in TEM for structure identification. The SAED has several advantages over *X-ray Diffraction* (XRD) and could be used complementarily with XRD. For instance, the specimen for SAED does not have to be a single crystal or even a polycrystalline powder. Plus, SAED can examine samples in areas as small as several hundred nanometers and thus can be used to analyze nanocrystals, interfaces, certain crystalline defects, and lattice parameters. TEM, HRTEM, and TEM diffraction were employed to observe NRGO and RGO in **Paper V** on FEI Titan Themis 200.

The *Atomic Force Microscopy* (AFM) is one high-resolution kind of scanning probe microscopes which use a cantilever with a probe to scan the surface of the sample. When the tip of the probe approaches the sample surface, the forces between the tip and sample deflect the cantilever.

AFM has two primary operation modes, namely contact mode and non-contact mode depending on whether the cantilever vibrates during the operation. In contact mode, the cantilever drags across the sample surface and it uses the deflection of the cantilever to measure the contours of the surface. In non-contact mode, the tip does not contact the surface of the sample and it is instead oscillated at a given frequency. A feedback loop system helps to maintain the oscillation amplitude constant by changing the distance from the tip to the sample. Recording the distance between the tip and sample at each point allows the software to construct a topographic image of the sample surface. AFM is conducted in non-contact mode to measure the thickness of graphene flakes produced by shear- and electrochemical exfoliation **in Paper I and II**.

3.3 Other characterization techniques

X-ray Diffraction (XRD) is a non-destructive analytical technique which relies on the dual wave/particle nature of X-rays and allows the phase identification within a crystalline material. When a beam of monochromated X-rays strikes a crystalline material, it will be scattered in all directions by the electron cloud surrounding the atoms in the material. The scattered X-rays will cancel one another out in most directions through destructive interference. But when Bragg's Law is satisfied, constructive interference of diffracted X-ray beams will occur (Figure 3.6). The Bragg's law is described by

$$n\lambda = 2d \sin \theta \quad (3.1)$$

where n = the diffraction order, λ = X-ray wavelength, d = the spacing between two crystal planes, and θ = the diffraction angle. By measuring the diffraction angles θ under which the diffracted X-rays constructively interfere, the interplanar spacings d of every single crystallographic phase can be determined. For unknown materials, by analyzing interplanar spacings d crystallographic phases could be determined.

X-rays are used to produce the diffraction pattern because their wavelength λ is typically the same order of magnitude (1–100 angstroms) as the spacing d between planes in the crystal. XRD was used to measure the spacing distance between GO and RGO layers (**Paper V**).

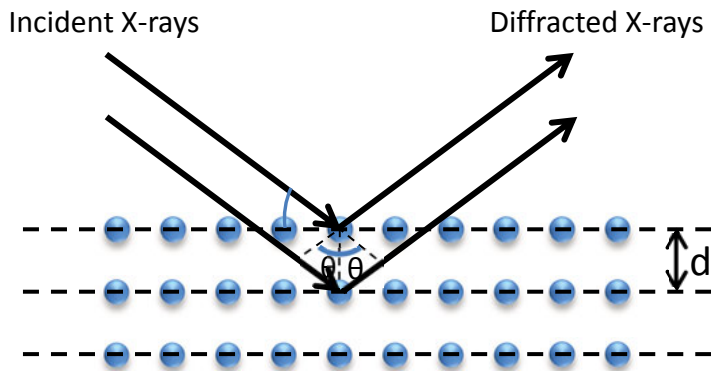


Figure 3.6 Illustration of diffraction of X-rays at a crystal.

Thermogravimetric analysis (TGA) is a technique in which the mass of a substance is monitored as a function of temperature or time as the sample specimen is subjected to a temperature program in a controlled atmosphere. The recorded temperature change provides information related to the physical and chemical phenomena involving mass change.[113] In this thesis, TGA was carried out for the measurement of silver content in reactive silver ink (**Paper II**), the thermal stability of GO and GO hydrogel (**Paper IV**), and the thermal stability of RGO and NRGO (**Paper V**). The instrument utilized is from TGA/SDTA 851e from Mettler Toledo, USA. Samples were placed into an alumina crucible under air flow (60 mL/min) and heated from 25 °C to 900 °C at a rate of 3 °C/min for GO or RGO based samples. For the measurement of Ag content in reactive silver ink, the sample was heated from 25 °C to 90 °C and kept at 90 °C for half an hour.

Rheological characterization

Viscosity is a measure of the resistance of fluid to an applied stress which is realized by a viscometer. Newtonian fluids exhibit constant viscosities at a specific temperature so they can be characterized by viscosity. Viscosity is a vital parameter for ink formation. In **Paper I to IV**, a commercial viscometer (Brookfield lvt viscometer, CIAB, chemical instrument AB) was used to measure the viscosity of the prepared graphene inks/dispersions.

In contrast, many materials exhibit changing viscosities as the strain rate changes, thus those are called non-Newtonian fluids. Rheology generally

accounts for the behavior of non-Newtonian fluids by studying the flow and deformation of materials under applied forces. The measurement of rheological properties is applicable to all materials from liquids to semi-solids such as pastes and creams, to solid polymers, to solids which under applied forces do not only deform elastically.

Viscoelastic materials exhibit both viscous and elastic characteristics when undergoing deformation. Such materials can be studied using dynamic mechanical analysis by applying a small oscillatory stress and measuring the resulting strain. Purely elastic materials have stress and strain in phase, so that the response of one caused by the other is immediate. In purely viscous materials, strain lags behind stress by a 90 degree phase lag. Viscoelastic materials exhibit behavior somewhere in the middle of these two types of material, exhibiting some lag in strain. Complex dynamic modulus G can be used to represent the relations between the oscillating stress and strain:

$$G = G' + iG'' \quad (3.2)$$

Where $i^2 = -1$, G' is the storage modulus and G'' is the loss modulus:

$$G' = \frac{\sigma_0}{\epsilon_0} \cos \delta \quad (3.3)$$

$$G'' = \frac{\sigma_0}{\epsilon_0} \sin \delta \quad (3.4)$$

where σ_0 and ϵ_0 are the amplitudes of stress and strain respectively, and δ is the phase shift between them.

The Rheological characterization was carried out on GO hydrogel and GO samples in **Paper IV** by AR2000 rheometer (TA Instruments, Inc., U.K.) with an 8 mm diameter aluminum plate at room temperature. GO hydrogel shows $G' > G''$, typical behavior of gels, whereas GO exhibits behavior between liquids and gels with $G' \approx G''$.

Electrical measurement

Four point probe method is a convenient tool to measure the electrical properties of a semiconductor or metal thin film. The four point probe method used in our measurement consists of four probes arranged linearly in a straight line at equal distance S from each other, as shown in Figure 3.7. During measurement, a constant current I is passed through the two outer probes and the potential drop V across the two middle probes is measured. When the sample is significantly larger (typically having dimensions 40 times greater) than the spacing of the probes, and the sample is thinner than 40% of the probe spacing, the sheet resistance can be calculated by[114]

$$R_s = \frac{\pi}{\ln(2)} \frac{V}{I} \approx \frac{V}{I} 4.5324 (\Omega / \square) \quad (3.5).$$

If the sample does not satisfy the condition, a correction factor based upon the geometry of the sample is required. This method was used to measure the electrical properties of printed patterns using our formulated graphene ink (**Paper I to III**).

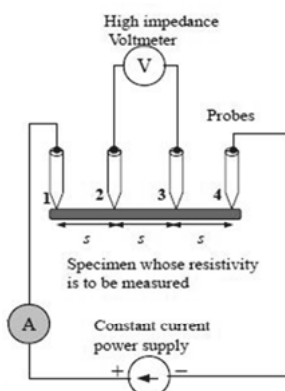


Figure 3.7 Illustration of the arrangements of four probes in a Four-probe setup.[115]

Electrocatalytic measurement

(Paper V) In order to measure the electrocatalytic ability of NRGO toward oxygen reduction reaction (ORR), the electrocatalytic measurements were carried out in a conventional three-electrode cell (as shown in Figure 3.8) using an IM6e electrochemical workstation (Zahner Elektrik, Germany) controlled at room temperature. Ag/AgCl (3.5 M KCl) and platinum foil were used as the reference and counter electrodes, respectively. A 5.0 mm diameter glassy carbon (GC) disk served as the substrate for the working electrode. The cyclic voltammetry (CV) tests were performed in N₂- and O₂-saturated 0.1 M aqueous KOH electrolyte solutions. Rotating disk electrode (RDE) tests were measured in O₂-saturated 0.1 M KOH at 1600 rpm with a sweep rate of 10 mV s⁻¹. In order to estimate the double layer capacitance, the electrolyte was deaerated by bubbling with N₂, and then the voltammogram was evaluated again in the deaerated electrolyte. The oxygen reduction current was taken as the difference between currents measured in the deaerated and O₂-saturated electrolytes.

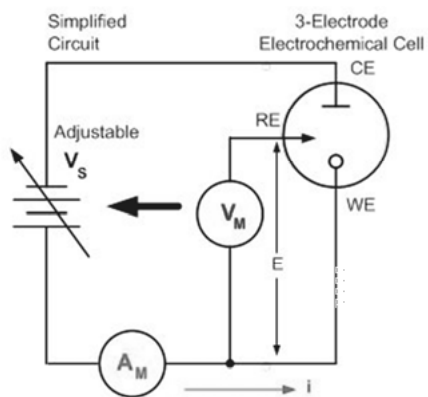


Figure 3.8 Simplified measurement circuit for cyclic voltammetry test. [116]

4. Overview of the appended papers

The excellent properties of graphene make it a promising candidate for conductive ink filler, but the potentials coexist with challenges. The reported graphene-based conductive inks show much poorer electrical properties than expected as shown in Table 1.3. In this thesis, different methods have been investigated for the preparation of highly conductive graphene inks for both inkjet and screen printing. Inkjet printing is the most convenient printing method for prototyping production, but it requires strict control over inks such as small size of graphene flakes, solvents with appropriate surface potential, and a specific range of ink viscosity. Therefore, small graphene flakes are prepared by exfoliation of graphite and then formulated into inks (Paper I and II). On the other hand, screen printing has less strict requirements for inks but requires much higher viscosity. Thus large-flake GO can be utilized. In order to enhance the electrical conductivity of GO based inks, GO dispersion is mixed with water-based reactive silver ink to make hybrid inks. The reduction condition for the GO/silver hybrid ink is subsequently studied (Paper III and additional results). The requirement of high viscosity for screen printing is satisfied by a gelation process (Paper IV). Inspired by the study on the GO gelation process, we demonstrate that ammonium formate possesses excellent reduction ability on GO, which is included in the latest manuscript (Paper V).

4.1 Graphene nano-platelet inks for inkjet printing

Background

A commercial Dimatix inkjet printer is available for the inkjet printing test and the typical cartridge nozzle has a diameter of 20 μm . Therefore, the ink filler, graphene flakes in our case, should be smaller than 1/20 of the nozzle diameter, which is 1 μm . In reality, the ink filler is much smaller than 1 μm in order to alleviate nozzle clogging problem. On the other hand, the concentration of ink filler should also be considered since it determines the printing efficiency. With those in mind, the shear- and electrochemical exfoliation of graphite are employed to prepare graphene flakes.

Experimental and results

The scalable shear exfoliation method has shown great potential for cost-effective mass production of pristine graphene. However, this method had not been utilized to prepare graphene inks before our work was done. In this work, we tested the shear exfoliation of graphite in three organic solvents i.e., ethanol, DMF, and NMP, all of which have similar surface energies to that of graphene. The best results were achieved in NMP and then formulated into inks. The thickness, surface roughness, transmittance, and conductivity of the printed films were studied versus printing passes, followed by the study on the properties as a function of annealing temperature. The main findings of this work (Paper I) include:

- Few-layer graphene nano-platelets (< 200 nm) are prepared by shear exfoliation of graphite in NMP. More than 60% of the graphene nano-platelets have thickness of ~ 2 nm, which corresponds to 4-layer graphene flakes.
- High-concentration (~ 3.2 mg/mL) stable graphene inks are formulated for inkjet printing by adding stabilizer ethyl cellulose and viscosity tuner ethylene glycol. Due to the high concentration, less printing passes are needed for a continuous film.
- The printed film exhibits the sheet resistance of $260 \Omega/\square$ with 86 % transmittance after annealing at 350°C for 2.5 hours, which is among the best reported performances in the literatures.
- The printed film shows superior flexibility and stability.

Electrochemical exfoliation of graphite in electrolyte provides another option for efficient production of graphene. The electrolytes are usually ionic liquids or water solutions of surfactants or inorganic salts. The water solutions of inorganic salts are comparatively inexpensive and easier to clean in subsequent processes. Thus in our case, $0.1 \text{ M } (\text{NH}_4)_2\text{SO}_4$ solution was used. Previous reports on electrochemically exfoliated graphene mostly consist of graphene flakes of large lateral size (several to tens μm) which are not suitable for inkjet printing. In our experiment, the parameters were tuned to prepare graphene nano-platelets. The exfoliated graphene nano-platelets were collected and redispersed in DMF to formulate inks with viscosity tuners ethylene glycol and glycerol. As-prepared graphene inks exhibited excellent stability even without any stabilizer, which was attributed to the small numbers of OFGs. The printing process was then studied versus printing passes and electrical properties were examined as a function of annealing temperature. The main findings of this work (Paper II) include:

- High-concentration (~ 2.8 mg/mL), few-layer graphene nano-platelets are prepared by electrochemical exfoliation of graphite. 80%

of the graphene nano-platelets have four layers showing an average thickness of ~ 2 nm.

- The exfoliated graphene nano-platelets can be readily dispersed in DMF without any stabilizer due to OFGs. With adding the viscosity tuners, the graphene inks are ready for inkjet printing.
- The as-prepared graphene nano-platelets share similarities with RGO that was reduced by annealing at 300 °C for two hours.
- The sheet resistance of printed film goes below $1 \text{ k}\Omega/\square$ with 53 % transmittance when annealed at 300 °C for 1 hour, which is still better than most of the reported results.

4.2 GO based inks for screen printing

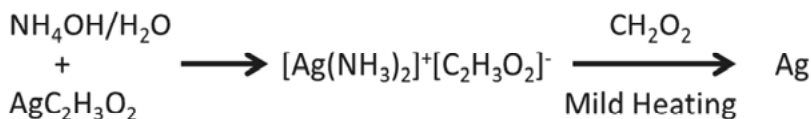
Background

While small flakes are necessary for inkjet printing, they introduce an increased number of flake-to-flake junctions in percolating films, which inevitably increase the resistivity of printed patterns. Plus, the high temperature annealing (up to 400 °C) will jeopardize the compatibility with flexible substrates and the toxic, high-boiling point solvents are not environment friendly. With those considerations, we carried out the study on GO based inks. As it is summarized in Table 1.3, GO based inks usually show inferior properties compared to graphene inks due to the reduction difficulty. To solve this, GO/silver hybrid ink is developed.

Experiments and results

Since GO dispersion is water based, so the water based reactive silver ink is chosen for the hybrid ink preparation. The reactive silver ink is prepared as reported[13] and the mechanism is shown in Scheme 4.1. Briefly, in the first step certain ammonium hydroxide (NH_4OH , liquid) is added to silver acetate ($\text{AgC}_2\text{H}_3\text{O}_2$, solid) to prepare silver ammonia ions $[\text{Ag}(\text{NH}_3)_2]^+$, which is the main component of Tollens' reagent. Subsequently, very little formic acid (CH_2O_2 , liquid) is added serving as reducing reagent for silver complexes. TGA analysis confirms that the silver content in the ink is around 20 wt%, shown in Figure 4.1.

Scheme 4.1 The preparation and reduction of reactive silver ink.



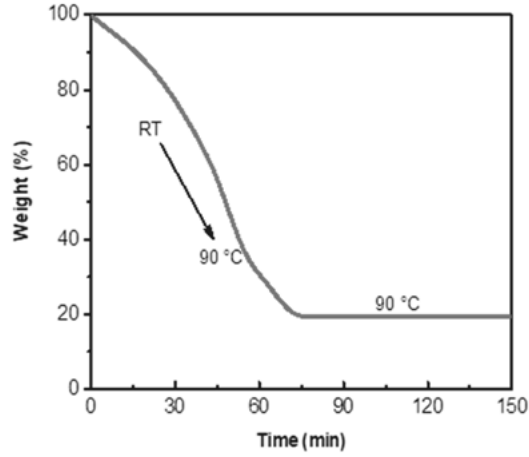


Figure 4.1 TGA curve of the prepared reactive silver ink.

In our experiment, the reactive silver ink was simply mixed with GO dispersion in different portion ratio. An immediate increase in the viscosity of the mixture was observed and made it ready for screen printing. The printed patterns were annealed at 160 °C for one hour to examine the annealing effect on the morphology and electrical performance. The annealed composites were denoted RGO/Ag_a (a represents the volume ratio of reactive silver ink to GO dispersion). XPS and XRD characterizations proved that the silver ions in the hybrid ink were reduced into metallic Ag after annealing. By this work (Paper III), we found:

- The electrical performances of RGO/Ag_a composites show inferior electrical conductivity relative to pure RGO and the conductivity decreases as the silver content increases.
- Further annealing the samples at 600 °C in reducing gas environment (Ar/H₂) though improves the overall conductivity of printed patterns, the RGO/Ag composites still show poorer electrical performance than RGO.
- The element analysis of RGO/Ag_a by XPS exhibits that as silver content in the composite increases, oxygen content increases accordingly.
- Based on the study, we propose that the reduced AgNPs in the RGO/Ag_a composites are covered by thin layer of AgO_x. The AgNPs are distributed between RGO layers, which results in enhanced contact resistance and deteriorate the overall electrical conductivity, as shown in Figure 4.2.

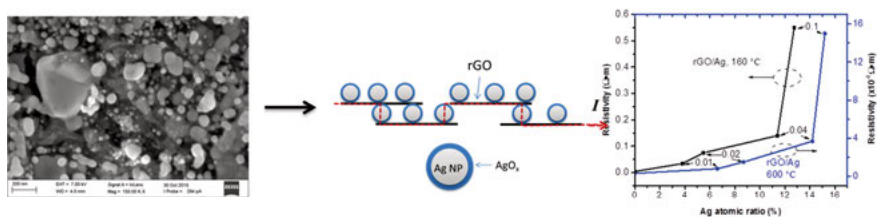


Figure 4.2 The $\text{AgO}_x\text{@AgNP}$ model for the RGO/Ag composites

Based on the above model, we further studied the annealing condition for such inks. Instead of annealing in air, we annealed printed patterns at 160 °C for two hours in Ar/H_2 in a quartz tube furnace. Take RGO/ $\text{Ag}_{0.02}$ as an example, the printed lines possess the similar laminated structure as RGO films while AgNPs were distributed between RGO layers (Figure 4.3).

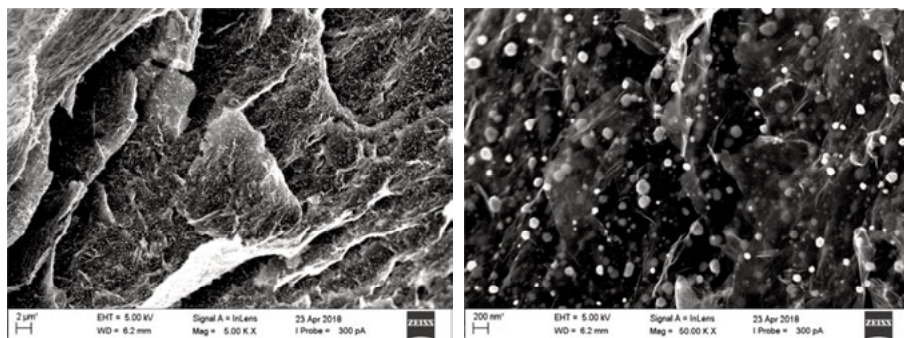


Figure 4.3 low (left panel) and high (right panel) magnification SEM pictures of RGO/AgNP composites.

The elemental analysis by XPS proved that as silver content increases, the oxygen content in the RGO/ Ag_a composites decreases and the C/O ratio increases (Figure 4.4). In other words, the existence of silver did not intervene but assisted the reduction of GO. As a result, the overall electrical performance was significantly improved, shown in Figure 4.5. The conductivity of RGO/ $\text{Ag}_{0.02}$ is around 250 S/cm (sheet resistance 30 Ω/\square) which is comparable to graphene films prepared from shear exfoliated graphene but only requires low temperature annealing and very low load of silver (< 0.1 wt%).

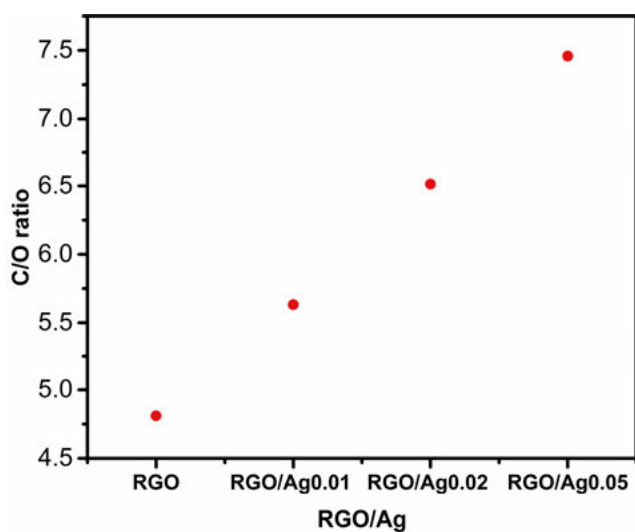


Figure 4.4 C/O ratios of RGO/Ag_a composites with increasing silver content after annealing at 160 °C in Ar/H₂ for two hours.

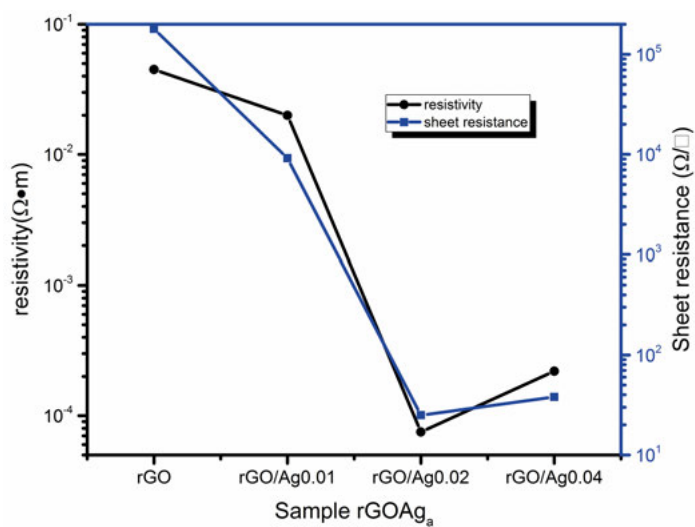


Figure 4.5 Resistivity and sheet resistance of as-prepared RGO/Ag composites by annealing at 160 °C in Ar/H₂ for two hours.

4.3 GO gelation

Background

The inks for screen printing require high viscosity, typically between 500-5000 cP. In the preparation of GO/Ag hybrid ink, it was found the viscosity increased instantly when reactive silver ink was added to GO dispersion, which made the mixture ready for screen printing. As a potential viscosity tuning approach, the chemical mechanism behind was studied in this work (Paper IV).

Experiment and results

The reactive silver ink consists of three ingredients, i.e., NH_4OH , CH_2O_2 , and $\text{AgC}_2\text{H}_3\text{O}_2$. $\text{AgC}_2\text{H}_3\text{O}_2$ can be dissolved in GO aqueous dispersion, while $\text{NH}_4\text{OH} + \text{AgC}_2\text{H}_3\text{O}_2$ will cause GO aggregation and precipitation instead of gelation. So $\text{AgC}_2\text{H}_3\text{O}_2$ is excluded for occurrence of the gelation. We examined the influence of NH_4OH , CH_2O_2 , and the combination of NH_4OH and CH_2O_2 on GO dispersion. It was found that the co-addition of NH_4OH and CH_2O_2 could induce instant gelation of GO aqueous dispersion with the aid of sonication, whereas each single chemical did not have such effect. The as-prepared GO hydrogel was thoroughly studied and we found that:

- The resultant GO hydrogel has higher C/O ratio and contains a small proportion of nitrogen as compared to GO.
- The carbonyl groups on GO sheets are removed and C-N bonds are generated in the gelation process.
- TGA analysis demonstrated the bonding changes in the GO system and the resultant GO hydrogel shows enhanced thermal stability.
- We propose that the additives (NH_4OH and CH_2O_2) react with carbonyl groups on GO sheets via Leuckart Reaction. This reaction results in de-oxygenation and amination of GO. Meanwhile, various bonding forces are generated within the GO system and thus viscosity increases, as illustrated in Figure 4.6.

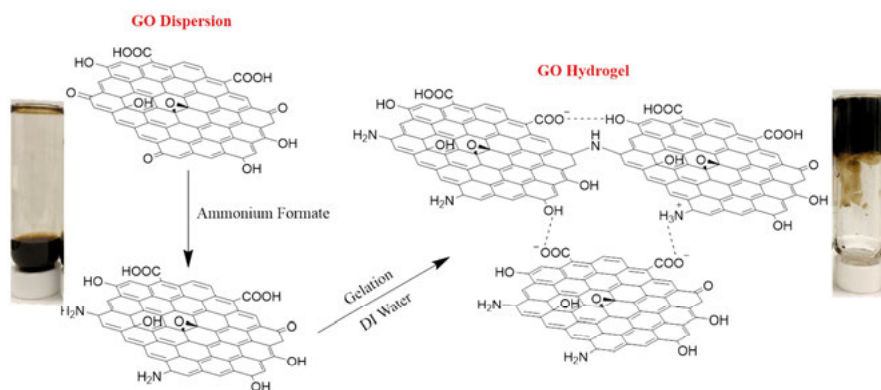


Figure 4.6 Illustration of gelation process of GO dispersion caused by ammonium hydroxide and formic acid.

4.4 GO reduction

Background

Reduction of GO is an important issue because we want to take advantage of the excellent liquid processability of GO on one hand, and expect the reduction could restore the outstanding properties of graphene, on the other. In the gelation of GO dispersion work, we found that ammonium formate possesses reducing and doping effect on GO even at room temperature. Thus we extended the study of GO reduction by hydrothermal method using ammonium formate as reducing reagent. Hydrothermal method is a common synthesis approach for production of RGO. One advantage of this method is that it is possible to produce 3D porous RGO macrostructures without any binders. The high surface area of RGO macrostructures together with the high conductivity makes it a promising candidate for electrodes in energy storage devices. However, the reduction ability of hydrothermal method is not good enough, so usually it is used together with reducing reagents.

Furthermore, nitrogen-doped carbon nanomaterials are proven efficient electrocatalysts for ORR which is an important half reaction in electrochemical energy conversion and storage systems such as fuel cells and metal–air batteries.[117] Therefore, the electrocatalytic ability of thus-prepared NRGO was also examined in this work.

Experiments and results

By using ammonium formate as reducing reagent GO was reduced and doped with nitrogen via hydrothermal method at 180 °C. The morphology of

resulting NRGO was examined by SEM and TEM. Besides, the reduction degree of resultant NRGO was also characterized by XPS, Raman, XRD, FTIR. It is found that:

- The NRGO presents a few-layer graphene interconnected 3D porous structure.
- The elemental analysis shows that the C/O ratio of NRGO is ~ 11 and ~ 5 at.% nitrogen atoms are incorporated into the RGO sheets. Under same condition, ammonium formate exhibits superior reduction ability for GO to L-ascorbic acid which is commonly used to prepare RGO.
- Most OFGs are removed in the reduction process but C-N bonds are generated.
- The cyclic voltammetry measurements proved that the NRGO exhibits excellent electrocatalytic ability for ORR as compared to RGO without nitrogen doping.

5. Concluding Remarks and Outlook

5.1 Concluding remarks

This thesis is based on the research work on conductive graphene-based inks for printed electronics applications. Specifically, two approaches were employed to reach the purpose. The first one is the preparation of graphene by exfoliation of graphite for inkjet printing. The main contribution includes applying the graphene-solvent surface energy theory to the graphene application and then the ink formulation. The second approach is the development of water-based GO/silver hybrid inks for screen printing. The contribution includes the experimental and theoretical study of the hybrid ink as well as the study of reduction ability of ammonium formate on GO.

The first step for the ink preparation is to obtain stable graphene-based dispersion. In Paper I, we tested the shear exfoliation of graphite in a range of solvents and achieved 4-layer graphene flakes when exfoliating graphite in NMP. In Paper II, electrochemically exfoliated graphene was dispersed in DMF. Graphene flakes could be stabilized in such solvents because the surface energies of those two solvents match that of graphene. In Paper III and the following unpublished work, we turned to water based GO dispersion and silver ink. The mixture of GO and silver ink was stabilized via a gelation process, which was discussed in Paper IV.

Another concern for ink preparation is the concentration of functional materials in the ink. It determines the printing efficiency and affects the quality of final printed structure. In our work, the functional materials are conductive components, graphene or RGO and Ag. By both shear- and electrochemical exfoliation methods, we achieved high concentration graphene dispersion. In GO/Ag hybrid ink, high concentration GO was mixed with silver ink to guarantee the amount of functional materials.

In addition, viscosity plays an important role in printing process. Inkjet printing requires viscosity in the range 10-20 cP for the best results whereas screen printing requires much larger viscosity (500-5000 cP). In Paper I, small amount of ethylene glycol was added to tune the viscosity of shear-exfoliated graphene dispersion. In Paper II, ethylene glycol and glycerol was added to enhance the viscosity because DMF has a much lower viscosity. The addition of viscosity tuner will dilute the concentration of functional materials in the ink and thus are undesired. In the preparation of GO/Ag hybrid ink (Paper III), co-addition of ammonium hydroxide and formic acid

(two important gradients for silver ink) would induce Leuckart reaction (a de-oxygenation reaction) on carbonyl groups on the edge of GO sheets, causing a gelation process. This gelation process instantly increases the viscosity of the resultant ink to the level suitable for screen printing (>1000 cP). It is worth noting that this method may be used to tune viscosity of GO based inks for other printing applications.

For GO-based inks, reduction is a decisive process for the final properties of printed patterns. In Paper III, thermal annealing, as an effective reduction method, was studied in terms of its effect on the electrical properties of the printed GO/Ag structures. We found that thermal annealing in air at relatively low temperature ($160\text{ }^{\circ}\text{C}$) brought in a higher electrical resistance of RGO/Ag composites due to the silver compound generated on the silver particles. However, annealing direct in reducing gas (Ar/H_2 5%) at the same temperature would solve this problem.

The finding of the reduction-induced gelation process in Paper IV inspired a further investigation of GO reduction. In the latest manuscript we studied the reduction of GO by hydrothermal method, in which ammonium formate, reaction product of ammonium hydroxide and formic acid, was used as the reducing reagent. We found that ammonium formate had very good reduction effect on GO. Furthermore, it showed that nitrogen atoms were incorporated into the carbon lattice of RGO sheets during the reduction, which made the resultant NRGO a promising candidate for electrocatalyst for ORR.

5.2 Outlook

The findings of this thesis work stimulate my thoughts about follow-up studies, such as:

1. Application of inkjet printing graphene inks to fabrication of electronic devices can be explored. Compared to other printing techniques, inkjet printing is easier to be integrated into a process chain.
2. For the GO/Ag hybrid ink, the reduction method may be further optimized. Screen printing of this material on flexible substrates, such as PI, can be expected subsequently. In addition, the effect of RGO in the composite, compared to silver, on the properties of printed patterns could be studied as well.
3. As a further study of Paper IV and V, hydrothermal synthesis of GO composites for electrocatalytic applications can be carried out.

Sammanfattning på svenska

Användandet av tryckkonsten för att tillverka elektronik möjliggör snabb och kostnadseffektiv tillverkning. Eftersom tillverkning av bläck kan placeras på en mängd olika material fungerar det även för flexibel elektronik. Tryckt elektronik finns idag både i vardagsprodukter och i industritillämpningar.

I all elektronik är ledarna mellan komponenterna viktiga. I tryckt elektronik är kraven att ledarna inte bara ska ha hög ledningsförmåga när de är på plats, de ska även ha goda egenskaper som bläck. Grafen, ett material bestående av ett eller några få lager kolatomer, har flera egenskaper som gör att det passar som funktionellt material i bläck till ledare. Det är ett flexibelt material med hög elektrisk ledningsförmåga och hög optisk transparens.

Målet med avhandlingsarbetet har varit att utveckla grafenbaserade bläck anpassade för att trycka elektriska ledare. För att skapa bläcket till tryckt grafenelektronik är det första steget att lösa upp grafenet i en vätska. Artikel I beskriver hur vi arbetade med mekanisk exfoliering av grafenlager från grafit till olika lösningsmedel. Vi fick bäst resultat med *N*-Methyl-2-pyrrolidone (NMP). Artikel II sammanfattar de fortsatta studierna med exfolierat grafen i lösningsmedel. Den här gången användes elektrokemiskt exfolierat grafen i dimetylformamid (DMF). Svårigheten med att lösa upp grafen i vätskor är att de enskilda flagorna attraheras av varandra och därför lätt klumpar ihop sig och faller ut. De här lösningsmedlen fungerar bra som lösningsmedel eftersom det har en ytenergi som matchar grafenets. Det minskar grafenets tendens till aggregering. Artikel III presenterar arbete med vattenbaserade grafenoxidlösningar med adderat silverbläck. Blandningen av grafenoxid och silverbläck stabiliserades genom en gelbildningsprocess. Den här gelbildningsprocessen diskuterades vidare i Artikel IV.

Om ett bläck ska bli användbart så är koncentrationen av funktionella material i det viktigt. Med funktionella material menas de material som ger bläcket dess funktion. I fallet med tryckt elektronik är funktionen elektrisk ledningsförmåga och de material som ger detta är i det här fallet grafen, reducerad grafenoxid, och silver. Genom både mekanisk och elektrokemisk exfoliering. I grafenoxid- och silverbläcket blandades höga koncentrationer av grafenoxid med silverbläck för att säkerställa att tillräckligt hög koncentration av de funktionella materialen kunde uppnås.

En annan viktig faktor för ett bläcks funktion är dess viskositet. Hur detta påverkar kan ses genom att studera hur en bläckstråleskrivare fungerar.

Bläcket suggs upp i ett rör som har en mynning som kan öppnas och stängas elektriskt. Den här mynningen flyttas till en punkt där en droppe bläck ska placeras och öppnas en kort stund så att en lagom stor droppe kan falla ner på underlaget. Om bläcket är för lättflytande så blir det mycket svårt att kontrollera droppstorleken medans om det istället är för trögflytande så kan det bli klumpbildning i röret och inget bläck kommer ut. För bläckstråleskrivning behövs en viskositet mellan 10-20 cP medan skärmtryck behöver en mycket högre viskositet på mellan 500-5000 cP. I Artikel I användes små mängder etylenglykol för att trimma in viskositeten av den mekaniskt exfolierade grafenlösningen. I Artikel II användes både etylenglykol och glycerol för att höja viskositeten då DMF har en lägre viskositet än NMP. Tillsats av vätskor för att trimma in viskositeten sänker koncentrationen av de funktionella materialen vilket är inte önskvärt. Vid tillverkningen av grafenoxid-silverbläcket tillsättes, ammoniumhydroxid och myrsyra som i rent silverbläck reducerar silverjoner till silver metall. Reagenom kan även reagera med grafenoxid i en s.k. Leuckhart-reaktion med karbonylgrupperna längs grafenoxidens kanter. Detta leder till en gelbildning som höjer viskositeten i bläcket till nivåer som passar skärmtryck ($cP > 1000$). Metoden kan även komma till användning för att ställa in viskositeten hos grafenoxidbläck till nivåer som passar andra tryckmetoder.

För att grafenoxidbläck ska bli ledande så måste grafenoxiden reduceras. I Artikel III utvärderas effekten av värmebehandling, även kallad "bakning" som reduceringsmetod, genom studier av hur de elektriska egenskaperna hos tryckta grafenoxid- och silverbläckstrukturer påverkas. "Bakning" i luft ledde även vid låga temperaturer till högre resistivitet eftersom silvret i bläcket oxiderades. När bakningen skedde i en atmosfär bestående av argon och väte så försvann detta problem då väte är reducerande.

Upptäckten att den reduktionsprocess som används i Artikel III även leder till gelbildning (Artikel IV) inspirerade oss till vidare undersökning, sista manuskriptet handlar om grafenoxid genom hydrotermiska processer. I dessa studier används ammoniumformiat, vilket är en reaktionsprodukt av ammoniumhydroxid och myrsyra, som reduktionsmedel. Vi upptäckte att ammoniumformiat hade en stark reducerande effekt på grafenoxid. Dessutom ledde den här processen till att kväveatomer byggdes in i grafenet vilket gav kvävedopad reducerad grafenoxid som är ett lovande katalysatormaterial.

Sammanfattningsvis har grafenbaserade bläck tagits fram och deras egenskaper har demonstrerats. Även om deras elektrisk ledningsförmåga är lägre än oorganiska bläck så är det en lovande väg framåt för billig elektronik.

Acknowledgement

This thesis is based on my research work in the past few years in Division of Solid State Electronics (FTE), Department of Engineering Sciences, Uppsala University. During my whole PhD life, I've received countless help and support from many people. So I would like to thank all of them from the bottom of my heart.

First of all, I would like to thank *Prof. Shili Zhang* and my main supervisor *Docent. Zhibin Zhang* for accepting me as a PhD student so that I had the chance to study in Sweden. I appreciate their help and support during my study.

Then I also sincerely thank *Prof. Helena Grennberg* who became my co-supervisor from the end of 2015. It is not only the knowledge but also the attitude toward research that I learned from her. I also want to cite another student of her "I admire your ability to see positive sides of every experiment or event, even when I was ready to interpret them as utter failures."

For *Prof. Jörgen Olsson*, it is not enough to say just thanks. I am so grateful for his generous help and support, for the fatherly advice. Also great thanks for his mentoring as an experienced teacher as well as skiing coach.

I worked in a small group but there were wonderful times. It is a pleasure to thank my former group members *Dr. Patrik Ahlberg* and *Dr. Malkolm Hin-nolm*, for their kind help on my experiments and languages, for those open-hearted and divergent talks, and for the laughs and complaints we shared. Big thanks to *Jie Zhao* for those warm talks and kind help on my experiments. Thanks to *Dr. Subima majee*, *Dr. Fengjuan Miao*, *Dr. Lars Riekehr* and *Dr. Leili Tahershamsi* for fruitful collaborations.

I also want to take this chance to thank *Xi Chen* for creating great memories together in Barcelona and Norway. I will cherish those memories. People say "You usually can't recall all the people you've shared laughs with. But you rarely forget the people you've shared your tears with." She is the kind that I've shared my tears with.

Thanks to *Tobias Törndahl* and *prof. Shili Zhang* (again) for commenting on this thesis.

Thanks to *Ingrid Ringård* for taking care of everything except research.

Sincere thanks to all *MSL staff* for keeping cleanroom running where more than half of the work was done, especially *Farhad* for taking care of our chemicals and *Amit* for his support for PVD machine, *Jan-Åke* for the help with XPS machine.

Thank *ALL FTE members* for great times and interesting Friday seminars, especially *Prof. Zhen Zhang*, *Dr. Xindong Gao*, *Dr. Si Chen*, *Dr. Lingguang Li*, *Dr. Shabnam Mardani*, *Lukas Jablonka*, *Katharina Rudisch*! Thank *Xingxing* and *Chenyu* for the help with my experiment.

Thank all my Chinese-speaking colleagues for making me less homesick!

As a PhD student in Solid Stated Electronics division who happened to be stuck in chemistry field, very often I had to seek help from outside the division. I was lucky and got help from lots of people, so I would like to give my deep thanks to all of them: *Dr. Ming Gao*, *Dr. Peng Zhang*, *Yuanyuan Han*, *Dr. Ken Welch* and *Dr. Jiaojiao Yang* (TGA), *Pedro Berastegui* (furnaces), *Dr. Hu Li* (XPS analysis discussion), *Dr. Seunghye Jong*, *Shenyang Zhou*, *Dr. Liyang Shi*, *Rui Sun*, *Dr. Ling Xie*, *Dr. Ruijun Pan*, *Dr. Zhaohui Xu* and many more.

I also owe my thanks to *my parents* for their unconditional love and support, *my brother and sister* for being there. Thank my parents in law for taking me as their own.

Thank all my friends for making life more fun!

Last but foremost, I couldn't thank enough my husband, *Da Zhang*, for accompanying me through those soul-crushing moments, for sharing joy and sorrow, for cooking delicious food, and most importantly, for being the one I love.

For those I have forgotten to mention names here. Extra thanks!

Reference

1. Printed electronics Market by Material (Inks and Substrates), Technology (Inkjet, Screen, Gravure, and Flexographic), Device (Sensors, Displays, Batteries, RFID tags, Lighting solutions/panels, and PV Cells), Industry, and Geography - Global Forecast to 2023.
2. Street, R.A., et al., Jet printing flexible displays. *Materials Today*, 2006. **9**(4): p. 32-37.
3. Gaikwad, A., et al., A flexible high potential printed battery for powering printed electronics. Vol. 6. 2013.
4. Kumar, R., et al., All-Printed, Stretchable Zn-Ag₂O Rechargeable Battery via Hyperelastic Binder for Self-Powering Wearable Electronics. *Advanced Energy Materials*, 2017. **7**(8): p. 1602096.
5. InfinityPV. 2018; Available from: <https://infinitypv.com/products/opv>.
6. Joshi, S., et al. Challenges and the state of the technology for printed sensor arrays for structural monitoring. in *SPIE Smart Structures and Materials + Non-destructive Evaluation and Health Monitoring*. 2017. SPIE.
7. Falco, A., et al., Fully Printed Flexible Single-Chip RFID Tag with Light Detection Capabilities. *Sensors (Basel, Switzerland)*, 2017. **17**(3): p. 534.
8. Wade, J., J.R. Hollis, and S. Wood, *Printed Electronics*. 2018, IOP Publishing.
9. Raghu Das, X.H., Khasha Ghaffarzadeh, *Flexible, Printed and Organic Electronics 2019-2029: Forecasts, Players & Opportunities*.
10. Ando, B., et al., Low-Cost Inkjet Printing Technology for the Rapid Prototyping of Transducers. *Sensors*, 2017. **17**(4).
11. Rajan, K., et al., Silver nanoparticle ink technology: state of the art. *Nanotechnology, Science and Applications*, 2016. **9**: p. 1-13.
12. Magdassi, S., M. Grouchko, and A. Kamyshny, Copper Nanoparticles for Printed Electronics: Routes Towards Achieving Oxidation Stability. *Materials*, 2010. **3**(9).
13. Walker, S.B. and J.A. Lewis, Reactive silver inks for patterning high-conductivity features at mild temperatures. *J Am Chem Soc*, 2012. **134**(3): p. 1419-21.
14. Wu, Y.L., Y.N. Li, and B.S. Ong, A simple and efficient approach to a printable silver conductor for printed electronics. *Journal of the American Chemical Society*, 2007. **129**(7): p. 1862-+.
15. Tao, Y., et al., A facile approach to a silver conductive ink with high performance for macroelectronics. *Nanoscale Research Letters*, 2013. **8**: p. 1-6.
16. Cuk, T., et al., Using Convective Flow Splitting for the Direct Printing of Fine Copper Lines. *MRS Proceedings*, 2011. **624**: p. 267.
17. Chang, Y., et al., Preparation, characterization and reaction mechanism of a novel silver-organic conductive ink. *Journal of Materials Chemistry*, 2012. **22**(48): p. 25296-25301.
18. Araki, T., et al., Cu Salt Ink Formulation for Printed Electronics using Photonic Sintering. *Langmuir*, 2013. **29**(35): p. 11192-11197.

19. Wallace, G.G., et al., Nanostructured carbon electrodes. *Journal of Materials Chemistry*, 2010. **20**(18): p. 3553-3562.
20. Lawes, S., et al., Printing nanostructured carbon for energy storage and conversion applications. *Carbon*, 2015. **92**: p. 150-176.
21. Moonen, P.F., I. Yakimets, and J. Huskens, Fabrication of Transistors on Flexible Substrates: from Mass-Printing to High-Resolution Alternative Lithography Strategies. *Advanced Materials*, 2012. **24**(41): p. 5526-5541.
22. Lim, S., et al., Inkjet-Printed Reduced Graphene Oxide/Poly(Vinyl Alcohol) Composite Electrodes for Flexible Transparent Organic Field-Effect Transistors. *Journal of Physical Chemistry C*, 2012. **116**(13): p. 7520-7525.
23. Wang, S., et al., High Mobility, Printable, and Solution-Processed Graphene Electronics. *Nano Letters*, 2010. **10**(1): p. 92-98.
24. Kong, D., et al., Temperature-dependent electrical properties of graphene inkjet-printed on flexible materials. *Langmuir*, 2012. **28**(37): p. 13467-72.
25. Zirkl, M., et al., An All-Printed Ferroelectric Active Matrix Sensor Network Based on Only Five Functional Materials Forming a Touchless Control Interface. *Advanced Materials*, 2011. **23**(18): p. 2069-+.
26. Huang, L., et al., Graphene-based conducting inks for direct inkjet printing of flexible conductive patterns and their applications in electric circuits and chemical sensors. *Nano Research*, 2011. **4**(7): p. 675-684.
27. Dua, V., et al., All-Organic Vapor Sensor Using Inkjet-Printed Reduced Graphene Oxide. *Angewandte Chemie-International Edition*, 2010. **49**(12): p. 2154-2157.
28. Le, L.T., et al., Graphene supercapacitor electrodes fabricated by inkjet printing and thermal reduction of graphene oxide. *Electrochemistry Communications*, 2011. **13**(4): p. 355-358.
29. Foster, C.W., et al., 3D Printed Graphene Based Energy Storage Devices. *Scientific Reports*, 2017. **7**: p. 42233.
30. Jeon, I., et al., Perovskite Solar Cells Using Carbon Nanotubes Both as Cathode and as Anode. *The Journal of Physical Chemistry C*, 2017. **121**(46): p. 25743-25749.
31. Stephen Lawes, Q.S., Xueliang Sun, *Handbook of Carbon Nano Materials*. 2015. 35.
32. Chen, J.H., et al., Intrinsic and extrinsic performance limits of graphene devices on SiO₂. *Nature Nanotechnology*, 2008. **3**(4): p. 206-209.
33. Perelaer, J., et al., Printed electronics: the challenges involved in printing devices, interconnects, and contacts based on inorganic materials. *Journal of Materials Chemistry*, 2010. **20**(39): p. 8446-8453.
34. Magdassi, S., M. Grouchko, and A. Kamyshny, Copper Nanoparticles for Printed Electronics: Routes Towards Achieving Oxidation Stability. *Materials*, 2010. **3**(9): p. 4626-4638.
35. Suganuma, K., *Introduction to Printed Electronics*. 2014. 148.
36. Novoselov, K.S., et al., Electric field effect in atomically thin carbon films. *Science*, 2004. **306**(5696): p. 666-669.
37. Frank, I.W., et al., Mechanical properties of suspended graphene sheets. *Journal of Vacuum Science & Technology B*, 2007. **25**(6): p. 2558-2561.
38. Castro Neto, A.H., et al., The electronic properties of graphene. *Reviews of Modern Physics*, 2009. **81**(1): p. 109-162.
39. Bolotin, K.I., et al., Ultrahigh electron mobility in suspended graphene. *Solid State Communications*, 2008. **146**(9-10): p. 351-355.

40. Virgin, L.N., Comment on "Mechanical properties of suspended graphene sheets" [J. Vac. Sci. Technol., B 25, 2558 (2007)]. Journal of Vacuum Science & Technology B, 2015. **33**(2).
41. Novoselov, K.S., et al., A roadmap for graphene. Nature, 2012. **490**(7419): p. 192-200.
42. Li, X.S., et al., Large-Area Synthesis of High-Quality and Uniform Graphene Films on Copper Foils. Science, 2009. **324**(5932): p. 1312-1314.
43. Kim, K.S., et al., Large-scale pattern growth of graphene films for stretchable transparent electrodes. Nature, 2009. **457**(7230): p. 706-710.
44. Gao, L.B., et al., Repeated growth and bubbling transfer of graphene with millimetre-size single-crystal grains using platinum. Nature Communications, 2012. **3**.
45. Reina, A., et al., Large Area, Few-Layer Graphene Films on Arbitrary Substrates by Chemical Vapor Deposition. Nano Letters, 2009. **9**(1): p. 30-35.
46. Mishra, N., et al., Graphene growth on silicon carbide: A review. physica status solidi (a), 2016. **213**(9): p. 2277-2289.
47. Tetlow, H., et al., Growth of epitaxial graphene: Theory and experiment. Physics Reports, 2014. **542**(3): p. 195-295.
48. Cai, M.Z., et al., Methods of graphite exfoliation. Journal of Materials Chemistry, 2012. **22**(48): p. 24992-25002.
49. Lotya, M., et al., Liquid Phase Production of Graphene by Exfoliation of Graphite in Surfactant/Water Solutions. Journal of the American Chemical Society, 2009. **131**(10): p. 3611-3620.
50. Hernandez, Y., et al., High-yield production of graphene by liquid-phase exfoliation of graphite. Nature Nanotechnology, 2008. **3**(9): p. 563-568.
51. Knieke, C., et al., Scalable production of graphene sheets by mechanical delamination. Carbon, 2010. **48**(11): p. 3196-3204.
52. Paton, K.R., et al., Scalable production of large quantities of defect-free few-layer graphene by shear exfoliation in liquids. Nature Materials, 2014. **13**(6): p. 624-630.
53. Chen, X.J., J.F. Dobson, and C.L. Raston, Vortex fluidic exfoliation of graphite and boron nitride. Chemical Communications, 2012. **48**(31): p. 3703-3705.
54. Yi, M. and Z. Shen, Kitchen blender for producing high-quality few-layer graphene. Carbon, 2014. **78**: p. 622-626.
55. Su, C.Y., et al., High-Quality Thin Graphene Films from Fast Electrochemical Exfoliation. Acs Nano, 2011. **5**(3): p. 2332-2339.
56. Liu, J.Z., et al., Electrochemically Exfoliated Graphene for Electrode Films: Effect of Graphene Flake Thickness on the Sheet Resistance and Capacitive Properties. Langmuir, 2013. **29**(43): p. 13307-13314.
57. Parvez, K., et al., Exfoliation of Graphite into Graphene in Aqueous Solutions of Inorganic Salts. Journal of the American Chemical Society, 2014. **136**(16): p. 6083-6091.
58. Wang, J., et al., High-Yield Synthesis of Few-Layer Graphene Flakes through Electrochemical Expansion of Graphite in Propylene Carbonate Electrolyte. Journal of the American Chemical Society, 2011. **133**(23): p. 8888-8891.
59. Vadukumpully, S., J. Paul, and S. Valiyaveetil, Cationic surfactant mediated exfoliation of graphite into graphene flakes. Carbon, 2009. **47**(14): p. 3288-3294.
60. Green, A.A. and M.C. Hersam, Solution Phase Production of Graphene with Controlled Thickness via Density Differentiation. Nano Letters, 2009. **9**(12): p. 4031-4036.

61. Hasan, T., et al., Solution-phase exfoliation of graphite for ultrafast photonics. *physica status solidi (b)*, 2010. **247**(11 - 12): p. 2953-2957.
62. Englert, J.M., et al., Soluble Graphene: Soluble Graphene: Generation of Aqueous Graphene Solutions Aided by a Perylenebisimide-Based Bolaamphiphile (*Adv. Mater.* 42/2009). *Advanced Materials*, 2009. **21**(42).
63. Guardia, L., et al., High-throughput production of pristine graphene in an aqueous dispersion assisted by non-ionic surfactants. *Carbon*, 2011. **49**(5): p. 1653-1662.
64. Khan, U., et al., High-Concentration Solvent Exfoliation of Graphene. *Small*, 2010. **6**(7): p. 864-871.
65. Secor, E.B., et al., Inkjet Printing of High Conductivity, Flexible Graphene Patterns. *The Journal of Physical Chemistry Letters*, 2013. **4**(8): p. 1347-1351.
66. Xu, L.X., et al., Production of High-Concentration Graphene Dispersions in Low-Boiling-Point Organic Solvents by Liquid-Phase Noncovalent Exfoliation of Graphite with a Hyperbranched Polyethylene and Formation of Graphene/Ethylene Copolymer Composites. *Journal of Physical Chemistry C*, 2013. **117**(20): p. 10730-10742.
67. Ou, E.C., et al., High concentration and stable few-layer graphene dispersions prepared by the exfoliation of graphite in different organic solvents. *Rsc Advances*, 2013. **3**(24): p. 9490-9499.
68. Li, J.T., et al., A simple route towards high-concentration surfactant-free graphene dispersions. *Carbon*, 2012. **50**(8): p. 3113-3116.
69. Li, J.T., et al., Efficient Inkjet Printing of Graphene. *Advanced Materials*, 2013. **25**(29): p. 3985-3992.
70. Zhao, W., et al., Preparation of graphene by exfoliation of graphite using wet ball milling. *Journal of Materials Chemistry*, 2010. **20**(28): p. 5817-5819.
71. Liu, N., et al., One - Step Ionic - Liquid - Assisted Electrochemical Synthesis of Ionic - Liquid - Functionalized Graphene Sheets Directly from Graphite. *Vol. 18*. 2008. 1518-1525.
72. Pei, S.F. and H.M. Cheng, The reduction of graphene oxide. *Carbon*, 2012. **50**(9): p. 3210-3228.
73. Valles, C., et al., Flexible conductive graphene paper obtained by direct and gentle annealing of graphene oxide paper. *Carbon*, 2012. **50**(3): p. 835-844.
74. Feng, Z.H., et al., Effect of high temperature treatment on the structure and thermal conductivity of 2D carbon/carbon composites with a high thermal conductivity. *New Carbon Materials*, 2014. **29**(5): p. 357-362.
75. Song, L., et al., Effect of high-temperature thermal treatment on the structure and adsorption properties of reduced graphene oxide. *Carbon*, 2013. **52**: p. 608-612.
76. Fernandez-Merino, M.J., et al., Vitamin C Is an Ideal Substitute for Hydrazine in the Reduction of Graphene Oxide Suspensions. *Journal of Physical Chemistry C*, 2010. **114**(14): p. 6426-6432.
77. Stankovich, S., et al., Synthesis of graphene-based nanosheets via chemical reduction of exfoliated graphite oxide. *Carbon*, 2007. **45**(7): p. 1558-1565.
78. Shin, H.J., et al., Efficient Reduction of Graphite Oxide by Sodium Borohydride and Its Effect on Electrical Conductance. *Advanced Functional Materials*, 2009. **19**(12): p. 1987-1992.
79. Zhu, C.Z., et al., Reducing Sugar: New Functional Molecules for the Green Synthesis of Graphene Nanosheets. *Acs Nano*, 2010. **4**(4): p. 2429-2437.
80. Pei, S.F., et al., Direct reduction of graphene oxide films into highly conductive and flexible graphene films by hydrohalic acids. *Carbon*, 2010. **48**(15): p. 4466-4474.

81. Liang, Y.T. and M.C. Hersam, Highly Concentrated Graphene Solutions via Polymer Enhanced Solvent Exfoliation and Iterative Solvent Exchange. *Journal of the American Chemical Society*, 2010. **132**(50): p. 17661-17663.
82. Secor, E.B., et al., Gravure Printing of Graphene for Large-Area Flexible Electronics. *Advanced Materials*, 2014. **26**(26): p. 4533-+.
83. Hyun, W.J., et al., High-Resolution Patterning of Graphene by Screen Printing with a Silicon Stencil for Highly Flexible Printed Electronics. *Advanced Materials*, 2015. **27**(1): p. 109-115.
84. Majee, S., et al., Scalable inkjet printing of shear-exfoliated graphene transparent conductive films. *Carbon*, 2016. **102**: p. 51-57.
85. Miao, F.J., et al., Inkjet printing of electrochemically-exfoliated graphene nanoplatelets. *Synthetic Metals*, 2016. **220**: p. 318-322.
86. Xiao, P., et al., Micro-contact printing of graphene oxide nanosheets for fabricating patterned polymer brushes. *Chem Commun (Camb)*, 2014. **50**(54): p. 7103-6.
87. Kim, J.H., et al., 3D Printing of Reduced Graphene Oxide Nanowires. *Advanced Materials*, 2015. **27**(1): p. 157-161.
88. Overgaard, M.H., et al., Highly Conductive Semitransparent Graphene Circuits Screen-Printed from Water-Based Graphene Oxide Ink. *Advanced Materials Technologies*, 2017. **2**(7).
89. Secor, E.B., et al., Rapid and Versatile Photonic Annealing of Graphene Inks for Flexible Printed Electronics. *Advanced Materials*, 2015. **27**(42): p. 6683-+.
90. Gao, Y.H., et al., Inkjet Printing Patterns of Highly Conductive Pristine Graphene on Flexible Substrates. *Industrial & Engineering Chemistry Research*, 2014. **53**(43): p. 16777-16784.
91. Huang, X.J., et al., Highly Flexible and Conductive Printed Graphene for Wireless Wearable Communications Applications. *Scientific Reports*, 2015. **5**.
92. Huang, X.J., et al., Binder-free highly conductive graphene laminate for low cost printed radio frequency applications. *Applied Physics Letters*, 2015. **106**(20).
93. Pei, L.M. and Y.F. Li, Rapid and efficient intense pulsed light reduction of graphene oxide inks for flexible printed electronics. *Rsc Advances*, 2017. **7**(81): p. 51711-51720.
94. Bourlinos, A.B., et al., Liquid-Phase Exfoliation of Graphite Towards Solubilized Graphenes. *Small*, 2009. **5**(16): p. 1841-1845.
95. Hossain, M.M., et al., High yield and high concentration few-layer graphene sheets using solvent exfoliation of graphite with pre-thermal treatment in a sealed bath. *Materials Letters*, 2014. **123**: p. 90-92.
96. Hughes, J.M., D. Aherne, and J.N. Coleman, Generalizing solubility parameter theory to apply to one- and two-dimensional solutes and to incorporate dipolar interactions. *Journal of Applied Polymer Science*, 2013. **127**(6): p. 4483-4491.
97. C. Schafhaeutl, *J. Prakt. Chem.*, 1840. **21**: p. 28.
98. B. C. Brodie, *Ann. Chim. Phys.*, 1855(45).
99. Hummers, W.S. and R.E. Offeman, Preparation of Graphitic Oxide. *Journal of the American Chemical Society*, 1958. **80**(6): p. 1339-1339.
100. Lerf, A., et al., Structure of graphite oxide revisited. *Journal of Physical Chemistry B*, 1998. **102**(23): p. 4477-4482.
101. Dave, S.H., et al., Chemistry and Structure of Graphene Oxide via Direct Imaging. *Acs Nano*, 2016. **10**(8): p. 7515-7522.
102. Kim, M.C., G.S. Hwang, and R.S. Ruoff, Epoxide reduction with hydrazine on graphene: A first principles study. *Journal of Chemical Physics*, 2009. **131**(6).

103. Gao, X.F., J. Jang, and S. Nagase, Hydrazine and Thermal Reduction of Graphene Oxide: Reaction Mechanisms, Product Structures, and Reaction Design. *Journal of Physical Chemistry C*, 2010. **114**(2): p. 832-842.
104. Jeong, H.K., et al., Thermal stability of graphite oxide. *Chemical Physics Letters*, 2009. **470**(4-6): p. 255-258.
105. Bagri, A., et al., Structural evolution during the reduction of chemically derived graphene oxide. *Nature Chemistry*, 2010. **2**(7): p. 581-587.
106. Wang, J.B., E.C. Salihi, and L. Siller, Green reduction of graphene oxide using alanine. *Materials Science & Engineering C-Materials for Biological Applications*, 2017. **72**: p. 1-6.
107. De Silva, K.K.H., et al., Chemical reduction of graphene oxide using green reductants. *Carbon*, 2017. **119**: p. 190-199.
108. Wang, H.L., et al., Solvothermal Reduction of Chemically Exfoliated Graphene Sheets. *Journal of the American Chemical Society*, 2009. **131**(29): p. 9910-+.
109. Liu, H.T., et al., Reduction of graphene oxide to highly conductive graphene by Lawesson's reagent and its electrical applications. *Journal of Materials Chemistry C*, 2013. **1**(18): p. 3104-3109.
110. Kumar, A. and M. Khandelwal, A novel synthesis of ultra thin graphene sheets for energy storage applications using malonic acid as a reducing agent. *Journal of Materials Chemistry A*, 2014. **2**(47): p. 20345-20357.
111. Thermo Scientific XPS. [cited 2013; Available from: <https://xpssimplified.com/elements/carbon.php>.
112. Stadtländer, C.T.K.-H. Scanning Electron Microscopy and Transmission Electron Microscopy of Mollicutes : Challenges and Opportunities. 2007.
113. Coats, A.W. and J.P. Redfern, Thermogravimetric Analysis. *Analyst*, 1963. **88**(105): p. 906-&.
114. Smits, F.M., Measurement of Sheet Resistivities with the Four-Point Probe. *Bell System Technical Journal*, 1958. **37**(3): p. 8.
115. vlab.amrita.edu. Resistivity by Four Probe Method. 2013; Available from: vlab.amrita.edu/?sub=1&brch=282&sim=1512&cnt=1
116. Tektronix. Performing Cyclic Voltammetry. 2015; Available from: <https://de.tek.com/blog/performing-cyclic-voltammetry>.
117. Zhang, J.T., Z.H. Xia, and L.M. Dai, Carbon-based electrocatalysts for advanced energy conversion and storage. *Science Advances*, 2015. **1**(7).

Acta Universitatis Upsaliensis

*Digital Comprehensive Summaries of Uppsala Dissertations
from the Faculty of Science and Technology 1780*

Editor: The Dean of the Faculty of Science and Technology

A doctoral dissertation from the Faculty of Science and Technology, Uppsala University, is usually a summary of a number of papers. A few copies of the complete dissertation are kept at major Swedish research libraries, while the summary alone is distributed internationally through the series Digital Comprehensive Summaries of Uppsala Dissertations from the Faculty of Science and Technology. (Prior to January, 2005, the series was published under the title "Comprehensive Summaries of Uppsala Dissertations from the Faculty of Science and Technology".)



ACTA
UNIVERSITATIS
UPSALIENSIS
UPPSALA
2019

Distribution: publications.uu.se
urn:nbn:se:uu:diva-377697